

# Multi-model assessment of the deglacial climatic evolution at high southern latitudes

Takashi Obase<sup>1,2</sup>, Laurie Menviel<sup>32</sup>, Ayako Abe-Ouchi<sup>1</sup>, Tristan Vadsaria<sup>134</sup>, Ruza Ivanovic<sup>54</sup>, Brooke Snoll<sup>54</sup>, Sam Sherriff-Tadano<sup>54</sup>, Paul J. Valdes<sup>65</sup>, Lauren Gregoire<sup>54</sup>, Marie-Luise Kapsch<sup>76</sup>, Uwe Mikolajewicz<sup>76</sup>, Nathaëlle Bouttes<sup>87</sup>, Didier Roche<sup>87</sup>, Fanny Lhardy<sup>87</sup>, Chengfei He<sup>98</sup>, Bette Otto-Bliesner<sup>109</sup>, Zhengyu Liu<sup>110</sup>, Wing-Le Chan<sup>1</sup>

<sup>1</sup>Atmosphere and Ocean Research Institute, The University of Tokyo, Kashiwa, Japan

<sup>2</sup>[Japan Agency for Marine-Earth Science and Technology, Yokohama, Japan](#)

<sup>32</sup>Climate Change Research Center, The Australian Centre for Excellence in Antarctic Science, the University of New South Wales, Sydney, Australia,

<sup>43</sup>UiT The Arctic University of Norway, Tromsø, Norway

<sup>54</sup>School of Earth & Environment, University of Leeds, Woodhouse Lane, Leeds, UK

<sup>65</sup>School of Geographical Sciences, University of Bristol, University Road, Bristol, UK

<sup>76</sup>Max Planck Institute for Meteorology, Hamburg, Germany

<sup>87</sup>Laboratoire des Sciences du Climat et de l'Environnement/Institut Pierre-Simon Laplace, UMR CEA-CNRS-UVSQ, Université Paris-Saclay, Gif-sur-Yvette, France

<sup>98</sup>~~Rosenstiel School of Marine, Atmospheric, and Earth Science, University of Miami, Miami, FL, USA~~  
[Woods Hole Oceanographic Institution, Woods Hole, MA, USA](#)

<sup>109</sup>Climate and Global Dynamics Laboratory, National Center for Atmospheric Research, Boulder, USA

<sup>110</sup>Atmospheric Science Program, Department of Geography, Ohio State University, Columbus, USA

Correspondence to: Takashi Obase ([obase@aori.u-tokyo.ac.jp](mailto:obase@aori.u-tokyo.ac.jp), [tobase@jamstec.go.jp](mailto:tobase@jamstec.go.jp))

**Abstract.** The quaternary climate is characterised by glacial-interglacial cycles, with the most recent transition from the last glacial maximum to the present interglacial (the last deglaciation) occurring between ~ 21 and 9 ka. While the deglacial warming at high southern latitudes is mostly in phase with atmospheric CO<sub>2</sub> concentrations, some proxy records have suggested that the onset of the warming occurred before the CO<sub>2</sub> increase. In addition, high southern latitudes exhibit a cooling event in the middle of the deglaciation (15 - 13 ka) known as the “Antarctic Cold Reversal” (ACR). In this study, we analyse transient simulations of the last deglaciation performed by six different climate models as part of the 4th phase of the Paleoclimate Modelling Intercomparison Project (PMIP4) to understand the processes driving high southern latitude surface temperature changes. [As the protocol of the last deglaciation sets the choice of freshwater forcing as flexible, the freshwater forcing is different in each model, thus hindering the multi-model comparison.](#) While proxy records from West Antarctica and the Pacific sector

of the Southern Ocean suggest the presence of an early warming before 18 ka, only half the models show a significant warming ( $\sim 1^{\circ}\text{C}$  or  $\sim 10\%$  of the total deglacial warming). All models simulate a major warming during Heinrich stadial 1 (HS1, 18 - 15 ka) ~~concurrent with the early warming, in response to the  $\text{CO}_2$  increase and with an AMOC weakening in some models. However, the simulated HS1 warming over Antarctica was smaller than the one suggested from ice core data. And simulations in which the AMOC weakens contributes to a more significant warming during HS1.~~ During the ACR, simulations with an abrupt AMOC increase exhibit a high southern latitude cooling during the ACR of 1 to  $2^{\circ}\text{C}$ , in relative agreement with proxy records, while simulations with rapid North Atlantic meltwater input exhibit a warming from Northern Hemisphere ice sheets exhibit opposite climate changes. Using simple models to extract the relative AMOC contribution, we find that all climate models simulate a high southern latitude cooling in response to an AMOC increase with a response timescale of several hundred years, suggesting the choice of the North Atlantic meltwater forcing substantially affects high southern latitudes temperature changes. Thus, further work needs to be carried out to reconcile the deglacial AMOC evolution ~~inferred from proxy records~~ with the ~~North Atlantic meltwater history inferred from ice sheet reconstructions~~ Northern hemisphere ice sheet disintegration and associated meltwater input. Finally, all simulations exhibit only minimal changes we do not find substantial changes in simulated Southern Hemisphere westerlies ~~and nor in the~~ Southern Ocean meridional circulation during ~~the last~~ deglaciation. Improved, suggesting the need to better understanding of the processes impacting southern high leading to changes in high southern latitude atmospheric and oceanic circulation changes accounting for as well as the processes leading to the deglacial atmospheric  $\text{CO}_2$  increase are needed.

## 1. Introduction

The recent Quaternary climate is characterised by glacial-interglacial cycles of about 100,000-year periodicity (Lisiecki and Raymo, 2005; Jouzel et al., 2007). These glacial-interglacial cycles are driven by insolation changes as external forcing and by feedbacks, including changes in atmospheric greenhouse gas (GHG) concentrations and ~~the waxing and waning of~~ continental ice sheets, ~~mainly in the northern high latitudes~~ (Abe-Ouchi et al., 2013). During the Last Glacial Maximum (LGM,  $\sim 21$  ka; ka indicates 1000 years before present), the continental ice sheets covered a significant area of the high

60 northern latitudes (Tarasov et al., 2012; Peltier et al., 2015), thus leading to a sea level fall of ~130 meters  
61 compared to pre-industrial (Lambeck et al., 2014). The atmospheric CO<sub>2</sub> concentration was also ~100  
62 ppm lower than ~~the~~ pre-industrial (Petit et al., 1999; Bereiter et al., 2015). These climatic boundary  
63 conditions contributed to a colder climate during the LGM, with global mean surface air temperature  
64 anomalies estimated to be  $4_{-5\pm0.9}^{+0.9}$  to  $7$  °C lower than present-day (Annan et al., 2022; [Liu et al., 2023](#)).  
65 As the last deglaciation (transition from the LGM to the early Holocene) represents one of the largest,  
66 most recent and well-documented natural warming of the last million years, an understanding of the  
67 processes and feedbacks during this time period can offer insight into our own modern changing world.  
68 Here, we focus on the high southern latitudes, where deglacial warming began before their Northern  
69 Hemisphere (NH) counterparts (Shakun et al., 2012), and which have been suggested to play a major role  
70 in driving the increase in atmospheric CO<sub>2</sub> concentration. Although the timing of the onset of the deglacial  
71 warming at high southern latitudes is poorly constrained, a compilation of Antarctic ice core records from  
72 East Antarctica suggested that the deglacial Antarctic warming started at ~ 18 ka, in phase with the rise  
73 in atmospheric CO<sub>2</sub> concentration (Parrenin et al., 2013). On the other hand, a record from the West  
74 Antarctic Ice Sheet Divide ice core (WDC) suggests that the warming started at ~ 20 ka (Shakun et al.,  
75 2012; WAIS project members, 2013). Moreover, an early onset of the deglacial warming (~21 ka) at [high](#)  
76 [and](#) mid-southern latitudes has also been suggested based on SST and sea ice records from the Pacific  
77 sector of the Southern Ocean (Moy et al., 2019; Sikes et al., 2019; Moros et al., 2021; Crosta et al., 2022;  
78 [Sadatzki et al., 2023](#)).

79       Millennial-scale climate events are superimposed on the deglacial warming. At the beginning of  
80 the deglaciation, during Heinrich stadial 1 (HS1, ~18 to 14.7 ka, following Ivanovic et al., 2016),  
81 Greenland and the North Atlantic region remained cold (Buizert et al., 2014, Martrat et al., 2007), while  
82 significant warming occurred at high southern latitudes (WAIS project members, 2010). This period was  
83 associated with a weakening of the Atlantic Meridional Ocean Circulation (AMOC), evidenced by Pa/Th  
84 in marine sediments (McManus et al., 2004; Ng et al., 2018). During the subsequent Bølling-Allerød (BA,  
85 ~14.7 to 12.8 ka) period, Greenland surface air temperatures rose by more than 10°C in just a few decades  
86 (Stephensen et al., 2008; Buizert et al., 2014), and the AMOC strengthened significantly (Severinghaus  
87 & Brook, 1999; McManus et al., 2004; Roberts et al., 2010; Ng et al., 2018). A cooling event at high

southern latitudes, known as the Antarctic Cold Reversal (ACR), was identified between ~15 and 13 ka (Jouzel et al. 2007; Pedro et al., 2016), concurrent with the BA. The Younger-Dryas (YD, 12.8 to 11.7 ka) followed the BA, and was characterised by a drastic cooling in Greenland and the North Atlantic. While the processes leading to the YD are still debated (Renssen et al., 2015), it has been suggested that the YD ~~could~~ be attributed to a weakening of the AMOC (McManus et al., 2004), caused by a rerouting of freshwater into the Arctic that was then transported toward the deep-water formation sites of the subpolar North Atlantic by coastal boundary currents (Condrón and Winsor, 2012; Kapsch et al., 2022). Climate model simulations with marine proxy constraints support the variations in the AMOC during the last deglaciation (Pöppelmeier et al., 2023).

An AMOC weakening causes a warming in the South Atlantic as the meridional oceanic heat transport to the North Atlantic is weakened (Stocker & Johnsen, 2003; Stouffer et al., 2006). This warming can then be propagated ~~in~~ to the Southern Ocean and Antarctica (Pedro et al., 2018). The contrasting temperature changes between Greenland and the southern high latitudes can also be found during abrupt events of the last ~~ice-age~~ deglacial period known as Dansgaard–Oeschger cycles (Dansgaard 1993; NGRIP project members, 2004; WAIS Divide project members, 2015), which have led to the notion of a bipolar seesaw (Stocker and Johnsen 2003; Capron et al., 2010). Alongside these events, the atmospheric CO<sub>2</sub> increase throughout the deglaciation occurred in steps, suggesting a link to millennial-scale climate events (Marcott et al., 2014) and changes in Southern Ocean circulation contributing to degassing of oceanic carbon (Anderson et al., 2009; Menviel et al., 2018).

Transient climate simulations provide a suitable framework for assessing the processes leading to deglacial climate changes. Early transient simulations that were conducted with transient orbital forcing, GHGs and ice sheets suggested that an increase in austral spring insolation in the southern high latitudes was responsible for the onset of warming (Timmermann et al., 2009), and that deglacial warming of the Southern Ocean appeared as early as ~20 to 18 ka in association with sea ice retreat (Roche et al., 2011). Transient simulations that also included freshwater input into the North Atlantic highlighted the AMOC impact on climate change (Liu et al., 2009; He et al., 2011). Menviel et al. (2011) further assessed showed that the ACR could be a response to the strong AMOC increase at the end of HS1, but that its length and amplitude could have been enhanced by meltwater input from the Antarctic ice sheet. ~~whether the ACR~~

~~was a response to the strong AMOC increase at the end of HS1 or whether it was caused by enhanced meltwater input from the Antarctic ice sheet.~~ These simulations were designed to simulate AMOC changes in agreement with estimates from proxy records, and therefore the magnitude, location, and timing of the implemented meltwater fluxes were idealised. In contrast, experiments forced with meltwater fluxes consistent with ice sheet reconstructions based on sea-level constraints often simulate millennial-scale AMOC changes in disagreement with accepted interpretations of climate and ocean records (Snoll et al., 2024). Some experiments simulate an AMOC weakening at the time of the BA because of significant mass loss of NH ice sheets (Bethke et al., 2012; Ivanovic et al., 2018a; Kapsch et al., 2022; Bouttes et al., 2023) or do not simulate any abrupt climate events (Gregoire et al., 2012). With an idealised scenario that follows the evolution of NH ice sheets more closely (except for the 14 ka meltwater pulse), the MIROC climate model shows that it is possible to simulate an abrupt AMOC strengthening with the presence of continuous freshwater in the North Atlantic because of gradual warming (Obase and Abe-Ouchi, 2019). These studies indicate that different models have different sensitivities in terms of the AMOC response to forcing and, therefore, it is useful to analyse multi-model results for a robust understanding of the climatic processes.

To facilitate further examination of the mechanisms driving deglacial climate change, a protocol for carrying out transient simulations of the last deglaciation was proposed as part of the fourth phase of the Paleoclimate Modeling Intercomparison Project (PMIP4) (Ivanovic et al., 2016). The protocol of PMIP4 deglaciation summarised climate forcings needed (ice core based atmospheric GHGs and reconstructed ice sheets) for climate model experiments. The protocol is designed to be flexible in that the use of some boundary conditions is determined by each modelling group, which allows an explorations of different climate scenarios. The first PMIP multi-model study of the last deglaciation, focusing on the northern hemispheric climate during HS1, found that different freshwater approaches (melt-uniform, melt-routed, trace-like, bespoke, Snoll et al. (2024)) have a dominant impact on North Atlantic climate variability. While this finding could be drawn due to the flexibility of the PMIP deglaciation protocol (Ivanovic et al., 20186) regarding the choice of the method on how to distribute the freshwater forcing, this flexibility makes it challenging to properly compare the simulations. Nevertheless, The multi-model assessment of the last deglaciation performed here provides an opportunity to

investigate the ~~mechanism-processes impacting southern high latitude climate~~ of past climate changes and to evaluate the uncertainties from the models' sensitivity to the forcings.

Some boundary conditions for climate models, including GHG and Antarctic ice sheet (prescribed in PMIP4 protocol), result from climate change at ~~the~~ high southern latitudes. [Proxy records \(Sigman et al., 2010, Skinner et al., 2010, Martinez-Garcia et al., 2011\)](#) and [modelling studies \(Bouttes et al., 2012, Menviel et al., 2016, Menviel et al., 2018, Gottschalk et al., 2019\)](#) ~~Proxy records and modelling studies~~ indicate that physical and biogeochemical changes in the Southern Ocean may have significantly contributed to ocean carbon uptake during ~~the last glacial periods and to, and that early deglacial changes in the Southern Ocean could have provided a major contribution to~~ the atmospheric CO<sub>2</sub> increase ~~observed~~ during HS1 ~~(Sigman et al., 2010, Skinner et al., 2010, Martinez-Garcia et al., 2011, Bouttes et al., 2012, Menviel et al., 2016, Menviel et al., 2018, Gottschalk et al., 2019)~~. Subsurface warming on the Antarctic shelf contributes to the mass loss of Antarctic ice sheets through enhanced melting of ice shelves, and retreat of grounding lines (Golledge et al., 2014; Lowry et al., 2019). In addition, climate conditions at high southern latitudes can impact the formation of ~~the~~ Antarctic Bottom Water (AABW) and the shoaling of AMOC (Sherriff-Tadano et al., 2023). Hence investigating the [deglacial](#) climate evolution at high southern latitudes may give an insight into critical climate system feedback ~~during the last deglaciation~~.

Here, we analyse the deglacial climatic evolution (21–11 ka) at high southern latitudes as simulated in six PMIP4 transient experiments, and compare the results with paleo-proxy records. ~~The first PMIP multi-model study of the last deglaciation focusing on the northern hemispheric climate during HS1 found that different freshwater approaches (melt routed, trace like, bespoke, Snoll et al. (2024)) have a dominant impact on North Atlantic climate variability. While this finding could be drawn due to the flexibility of the PMIP deglaciation protocol (Ivanovic et al., 2018) regarding the choice of the method on how to distribute the freshwater forcing, this flexibility makes it challenging to properly compare the simulations. Nevertheless, a comparison of six climate models gives the opportunity to assess the magnitude of a climate warming or cooling, which is here carried out with help of simple models and the analysis of additional sensitivity experiments.~~ We [mainly](#) focus on the [magnitude and rate of](#) Antarctic surface air temperature (SAT) and Southern Ocean sea surface temperature (SST) changes. As there is a substantial difference between the AMOCs in the simulations, we utilise statistical or simple models to



~~assess-separate~~ the impact of changes in atmospheric CO<sub>2</sub> and AMOC on Southern Ocean SST. ~~We~~  
~~Finally, we~~ analyse the evolution of the AABW, Southern Ocean westerlies and subsurface ocean  
temperature in the Southern Ocean to discuss critical climate system feedbacks occurring at high southern  
latitudes.

## 2 Methods

### 2-1 Climate models and experiments used in this study

We use the PMIP4 transient simulations of the last deglaciation performed with six atmosphere-ocean coupled climate models ~~(Table 1)-(Table 4)~~. ~~Table 2 summarises the experimental design of each model simulation and their reference articles, with These simulations are taken from the respective published article displayed in Table 2, and the evaluation using of their LGM and PI states is found from mentioned in their description.~~ These simulations are initialised with ~~LGM-glacial~~ conditions, ~~and the LGM climate fields have been evaluated by previous studies, particularly for global temperature changes (Kageyama et al. 2021), sea ice and SST changes in the Southern Ocean (Lhardy et al., 2021; Green et al. 2022), and SAT changes over the Antarctic ice sheet (Buizert et al. 2021). A part of the transient simulations utilized in this study have also been compared to proxy-reconstructions (Weitzel et al. 2024). Fig. S1 compares simulated sea-ice edges for the pre-industrial simulations from six models used in this study, which shows models simulate reasonable sea ice extents.~~ The Equilibrium Climate Sensitivity (ECS, defined by global mean SAT changes in response to doubling CO<sub>2</sub> from the pre-industrial) of each model ranges from 2.0 to 3.9 °C, and the global mean surface air temperature (SAT) anomaly for the LGM is 3.5 to 7.3 °C (Table 1). ~~Table 2 summarises the experimental design of each model simulation and their reference articles.~~ While some of the modelling groups performed two or more sensitivity experiments with different model parameters or boundary conditions (e.g., different freshwater forcing (FWF) scenarios or ice sheets), for this study we have selected one representative simulation from each climate model. Fig. 1 summarises the time evolution of the climate forcings, i.e. insolation, atmospheric GHGs, and continental ice sheets used in the simulations. Both reconstructions (ICE-6G\_C VM5a, henceforth ‘ICE-6G\_C’; and ‘GLAC-1D’) have larger Antarctic ice sheet volume at the LGM, with a ~ 10 m sea-level equivalent volume change at the LGM, relative to present-day. Both suggest ~

100 m of elevation change since the LGM at EPICA Dome C (EDC, 123°E, 75°S), while WAIS Divide (WDC, 112°W, 79.5°S) differs by 300 meters between the two datasets (Fig. 1d).

Fig. 2a summarises the total amount of FWF in the NH in six simulations. The FWF schemes can be classified into two groups: [a] FWF adjusted to reproduce large-scale AMOC variability (iTRACE, LOVECLIM, MIROC) and [b] FWF consistent with the reconstructed ice volume changes (HadCM3, MPI-ESM, iLOVECLIM) based on ICE-6G\_C or GLAC-1D (Fig. 2a, black lines). Notably, during HS1, iTRACE and LOVECLIM have significant FWF (~ 0.2 Sv), while other simulations apply FWF of less than 0.1 Sv. In LOVECLIM and MIROC, the meltwater flux was uniformly applied to the North Atlantic, while other models use the location of the melting NH ice-sheet and associated runoff to apply a spatially varying FWF (Table 2). ICE-6G\_C (HadCM3, MPI-ESM, iLOVECLIM) leads to a meltwater input of about 0.1 Sv to the Southern Ocean at 11.5–11 ka. iTRACE and LOVECLIM also applied freshwater flux to the Southern Ocean to simulate the ACR (iTRACE: up to 0.2Sv during 14.4–13.9 ka, LOVECLIM: fixed at 0.09Sv during 14.67–14.1 ka).

In section 3.3, we conduct further analysis to examine the processes driving Southern Ocean SST using a multilinear regression (MLR) model and a thermal bipolar seesaw model adapted from Stocker and Johnsen (2003).

## 2-2: Simple models to disentangle CO<sub>2</sub> and AMOC

### 2-2-1: Multilinear Regression model

We use a MLR model to regress changes in SST onto CO<sub>2</sub> and AMOC variations:

$$SST = \alpha_I * CO_2 + \beta_I * AMOC + \gamma, (1)$$

where ~~SST (Southern Ocean SST, averaged over 55–40°S)~~, and *AMOC* (defined as the maximum meridional overturning streamfunction in the North Atlantic, at depths below 500 m and 20–60°N) are output from the climate models, and *CO<sub>2</sub>* is the forcing used in each simulation.  $\gamma$  is the intercept. The AMOC in the analysis is normalised with respect to the maximum and minimum values in each model. The CO<sub>2</sub> is also normalised with respect to the total change between 21 and 11 ka (~83 ppm). The MLR analysis is applied to the ~~time-varying areally-averaged Southern Ocean SST values and time-varying 2-D fields of the Southern Ocean SST, respectively.~~ The same analysis is applied to the Southern Ocean



SST averaged over 55–40°S. Every 100-years, mean SST, AMOC, and CO<sub>2</sub> from 20 to 11 ka are used as the input for this analysis, so each dataset has 90 time-slices. While we use CO<sub>2</sub> as a representation of a gradual forcing as the input of the MLR model, we note that other forcing, such as from ice sheets and orbital changes can contribute to the warming. On the other hand, sensitivity experiments evaluating the contribution of each forcing shows that they have a minor impact on Southern Ocean SST and Antarctic SAT changes during between 19 and 15 ka (He et al. 2013). One note is that we do not consider insolation nor other forcings, because the insolation forcing and CO<sub>2</sub> are not independent; both gradually change during the last deglaciation (Fig. 1).

## 2-2-2: Thermal bipolar seesaw model

As the MLR model does not consider transient climate response, we construct a thermal bipolar seesaw model following Stocker and Johnsen (2003). The original thermal bipolar seesaw model is based on an energy balance between the North and South Atlantic Oceans. We add the effect of CO<sub>2</sub> on temperature, which was not considered in the original model. The thermal bipolar seesaw model in this study solves the temporal evolution of Southern Ocean SST using the following equations:

$$\frac{d\Delta SST}{dt} = \frac{\Delta SST_{eq} - \Delta SST(t)}{\tau} \quad (2)$$

$$\Delta SST_{eq} = \alpha_2 * CO_2(t) + \beta_2 * m(t) \quad (3)$$

where  $\Delta SST_{eq}$  is an equilibrium temperature Southern Ocean SST (change since the LGM) expected from the CO<sub>2</sub> and state of the AMOC at time  $t$ .  $\Delta SST(t)$  is the SST change since LGM at time  $t$ , and  $\tau$  is the characteristic timescale of the bipolar seesaw.  $CO_2(t)$  is the CO<sub>2</sub> concentration at time  $t$ , and is normalised with maximum and minimum values as in the MLR model. The term  $m(t)$  represents the modes of the AMOC ~~(strong or weak)~~ from the climate model outputs. When using the simulated AMOC within the bipolar seesaw model, it is assumed that the AMOC has only two modes, unlike the continuous values in the model. Based on Figure 2, we assume that the AMOC is in a strong mode ( $m(t)=0$ ) if the AMOC is greater than 14 Sv. Based on AMOC values in each model, we assume  $m(t)=0$  if the AMOC is greater than 14 Sv, and  $m(t)=1$  if the AMOC is smaller than 14 Sv.

~~Every 100-year mean AMOC and CO<sub>2</sub> value from 20 to 11 ka are used as the input, as the time step is set to 100 years. At first, we conduct systematic sensitivity experiments to calculate the minimum root mean square error between the actual  $\Delta SST$  and the bipolar seesaw models. We conduct 9610~~

sensitivity experiments for each model within the parameter ranges shown in Table 3. The combination of parameters that gives the minimum root mean square error, along with coefficient of determination between the climate models' SST changes and bipolar seesaw models are displayed in Table 5. The thermal bipolar model is initialised with SST=0. We investigate the best combinations of parameters ( $\alpha$ ,  $\beta$ ,  $\tau$ ) based on systematic sensitivity experiments, with combinations of parameters shown in Table 3 (9610 set of parameters for each model). We find the best combinations of parameters based on a minimum root mean square error estimator applied to simulated and actual SST changes in each model.

### 3. Results

#### 3-1: AMOC

As AMOC variations can impact southern high latitude climate, we summarise here the transient evolution of the AMOC in the different simulations. As detailed below, the AMOC evolution is substantially affected by the FWF schemes. All simulations except for MIROC display a strong ( $\sim 20$  Sv) AMOC at the LGM (Fig. 2b), while MPI-ESM and iLOVECLIM shows slightly weaker LGM AMOC if GLAC-1D ice sheet was used (Kapsch et al., 2022; Bouttes et al., 2023). The more vigorous LGM AMOC than the compared to Pre-Industrial (PI) is in line with the majority of PMIP4 simulations that display stronger AMOC at the LGM than during Pre-Industrial (PI; Kageyama et al., 2021), although it is not consistent with LGM reconstructions from multiple marine tracers (Lynch-Stieglitz et al., 2007; Bohm et al., 2015; Menviel et al., 2016). During the period corresponding to HS1, the AMOC stays weak in MIROC and significantly declines in the iTRACE and LOVECLIM simulations, as meltwater is added into the North Atlantic. On the other hand, in the other simulations, there is only a slight reduction in AMOC ( $\sim 1$  Sv) as the meltwater input into the North Atlantic stays below 0.05 Sv. At the BA ( $\sim 14.7$  ka), three models exhibit an abrupt change from weak to strong AMOC, triggered by a rapid reduction in FWF (iTRACE and LOVECLIM) or as a response to the gradual background warming (MIROC). These simulations, featuring an AMOC strengthening, broadly agree with marine proxy records (Fig. 2b black line). On the other hand, the other three simulations (HadCM3, MPI-ESM, iLOVECLIM) display an AMOC weakening due to a significant increase in FWF originating from the ice sheet collapse associated with Meltwater Pulse 1a (Deschamps et al., 2012). During the Younger-Dryas (12.8–11.7 ka), iTRACE,

LOVECLIM, and MIROC simulate an AMOC decline, corresponding to an increase in FWF or an oscillatory nature of the AMOC in MIROC (Kuniyoshi et al., 2022). HadCM3 simulates a gradual AMOC reduction, while MPI-ESM exhibits multi-centennial AMOC variability. At 11 ka, the AMOC strength returns to a strong mode except for iLOVECLIM, which stays weak after the BA.

### 3-2 SST and SAT

#### 3-2-1: 21–18 ka (onset of warming) and 18–14.7 ka (HS1)

Fig. 3 summarises the simulated Antarctic SAT and Southern Ocean SST changes since the LGM in all the simulations (LGM is defined as 21 ka in most models, with some exceptions because of differences in the timing of initialisation; 20.6 ka for LOVECLIM, 20.0 ka for iTRACE). The SAT at WDC and EDC are compared with the ice core based reconstructions from Parrenin et al. (2013) and Buizert et al., (2021).

#### 3-2-1: 21–18ka (onset of warming)

~~This period corresponds to mostly stable atmospheric CO<sub>2</sub>, with an increase in spring to summer insolation at southern high latitudes driven primarily by obliquity change (Fig. 1a).~~ Three models (MIROC, HadCM3, MPI-ESM) exhibit a gradual ~1°C warming between 21 and 18 ka at both WDC and EDC (Fig. 3c). This simulated EDC warming is comparable with EDC ice core estimates (Parrenin et al., 2013). However, the magnitude of warming suggested from WDC (~2°C warming between 19.5–19 ka, Shakun et al., 2012) is not simulated by any of the models, with iTRACE exhibiting slight cooling (Fig. 4a). ~~On the other hand, a slight cooling is simulated at WDC in iTRACE and at EDC in LOVECLIM, with the latter exhibiting little change (Fig. 4a).~~

~~Significant SAT warming in~~ MIROC, HadCM3 and MPI-ESM also simulate a significant SAT increase over Antarctica and occurs at the same time as a 0.5–1.0°C SST warming increase in the Southern Ocean north of the sea ice edge, and with a gradual reduction in Southern Ocean sea ice area (Figs. 3f and 4).

#### 3-2-2: 18–14.7ka (HS1)

~~This period corresponds to an increase in CO<sub>2</sub> from 190 to 230 ppm. Reconstructions from the WDC and EDC suggest a 4–8°C warming (Fig. 3c–d).~~ All models exhibit a larger warming during this

~~period than~~ between 18 and 14.7 ka (i.e. HS1) ~~than~~ between 21 and 18 ka. iTRACE simulates the largest warming (+6–8°C), closely following the estimates from ice core data. The sharp increase in temperature in iTRACE starts at ~18 ka, corresponding to a period of major reduction in AMOC strength (Fig. 3b). The warming in MPI-ESM follows iTRACE with a 5°C warming, despite a minor reduction in AMOC strength. The HadCM3 exhibits ~4°C warming at WDC and ~2°C warming at EDC, while the other models simulate a 2–4°C warming at EDC and WDC (Fig. 3c–d). iTRACE exhibits the most significant Southern Ocean SST ~~warming a~~increase of 5 °C and LOVECLIM exhibits a sharp Southern Ocean SST increase ~~of~~ ~3°C, in response to an AMOC reduction at ~17 ka. The other models' Southern Ocean SST increase by 1–2 °C (Fig. 3e). Southern Ocean sea ice area exhibits the same trends as the Southern Ocean SST, with iTRACE simulating the largest sea ice area reduction of up to 40% compared to the LGM (Figs ~~3f~~ and 4b).

### **3-2-~~23~~: 14.7–13 ka (BA) and 13–11 ka (YD and Holocene onset)**

~~At 14.7 ka the abrupt and large warming of the BA is recorded in Greenland, while a gradual 2°C cooling (ACR) is recorded at WDC and EDC between 14.7 and 13 ka.~~ Three models (iTRACE, MIROC, LOVECLIM) simulate an abrupt AMOC increase at the BA onset, and a concomitant cooling at high southern latitudes: ~1-2 °C Antarctic SAT and Southern Ocean SST decrease. iTRACE and LOVECLIM exhibit a sharp cooling in Southern Ocean SST and SAT in the early phase of the BA, probably enhanced by the meltwater flux into the Southern Ocean (Menviel et al., 2011). In contrast, the three other models (HadCM3, MPI-ESM, iLOVECLIM) exhibit a warming in the early phase of the BA, corresponding to an AMOC weakening. Subsequently, HadCM3 and MPI-ESM exhibit a gradual cooling over the Antarctic and Southern Ocean as the AMOC strengthens in the later part of the BA (~13.5 ka). iLOVECLIM displays a rapid warming at 13.5 ka, followed by a cooling ~~despite the AMOC being weak throughout this period~~, which is explained by abrupt surface albedo changes caused by the evolving land-sea mask in the Antarctic region (Bouttes et al., 2023).

### **~~3-2-4: 13–11ka (YD and Holocene onset) and total deglacial warming~~**

~~This period corresponds to the~~During YD (13–11ka), ~~during which an AMOC weakening has been suggested (McManus et al., 2004, Ng et al., 2018). Both EDC and WDC reconstructions show a 2–4°C warming between 13 and 12 ka. During that time,~~ iTRACE, MIROC, and LOVECLIM simulate an

AMOC weakening as well as a high southern latitude warming. iTRACE simulates a  $\sim 3\text{--}4^\circ\text{C}$  increase in Southern Ocean SST, while LOVECLIM and MIROC simulate a  $1^\circ\text{C}$  warming. MPI-ESM exhibits multi-centennial variability associated with variations in AMOC strength. MPI-ESM and iLOVECLIM exhibit sharp cooling in Southern Ocean SST and SAT starting at  $\sim 11.5$  ka, enhanced by the meltwater flux into the Southern Ocean (Kapsch et al., 2022).

The total deglacial (21–11 ka) warming is  $10^\circ\text{C}$  in WDC, while the EDC estimates range from 5 to  $10^\circ\text{C}$  (Parrenin et al., 2013; Buizert et al., 2021). Across the simulations, a 2 to  $10^\circ\text{C}$  warming is simulated over Antarctica. ~~Only one model (MPI-ESM) simulates a larger warming at EDC than at WDC, while three models suggest a larger temperature change at WDC (iTRACE, HadCM3, LOVECLIM), and two models show a similar warming at both sites (MIROC, iLOVECLIM).~~ In line with the WDC and the upper range of EDC estimates, iTRACE and MPI-ESM display a  $8\text{--}10^\circ\text{C}$  total warming over Antarctica. The Southern Ocean sea ice edge retreats poleward by  $10^\circ$  latitude in most models. A SST increase of up to  $6^\circ\text{C}$  is simulated in this area in iTRACE, LOVECLIM, HadCM3, and MPI-ESM, while a  $\sim 4^\circ\text{C}$  SST increase is simulated in MIROC and iLOVECLIM (Fig. 5).

The different magnitudes of warming during HS1 and YD between models could be explained by the range of temperature changes between LGM and PI, as the mean SAT and SST changes are different by a factor of two (Table 1). To reduce this model difference, Antarctic SAT are normalised by the temperature anomaly between LGM and PI in Figure 6. When normalised, the simulations with a weak AMOC during HS1 show the largest warming over Antarctica (Fig. 6 left). ~~iTRACE still has the largest warming (Fig. 6a), MIROC and LOVECLIM display the second and third largest warming for HS1. One common point in these three models is the weak AMOC in HS1 (Fig. 6b left). Even if the total amount of global warming is small, the weakening of AMOC in HS1 with MIROC and LOVECLIM contributes to HS1 warming as in iTRACE. In contrast, the other three models (HadCM3, MPI-ESM, and iLOVECLIM) exhibit mostly strong AMOC during HS1, and the normalised HS1 warming were smaller (Fig. 6 right panels).~~ The normalised Antarctic SAT change at 11 ka varies lies in between 0.63– and 0.8 with respect to the total temperature change between LGM and PI for five out of six models, indicating. This indicates that ~~some~~ warming ~~also~~ occurred after the onset of the Holocene. This, which marks a ~~main~~ difference

between the simulations and proxy data, in that the temperature at 11 ka is comparable to the pre-industrial values based on ice core reconstructions (Parrenin et al., 2013; Buizert et al., 2021).

### 3-3: SST – CO<sub>2</sub> – AMOC relationship analysis

The simulated AMOC time series display large differences across simulations ~~derived from~~due to different FWF schemes, which complicates the quantification of ~~the relative importance of~~ CO<sub>2</sub> forcing and AMOC changes in driving high southern latitude temperature changes in each model. To overcome this, we examine the Southern Ocean SST trajectory against CO<sub>2</sub> forcing, and AMOC strength (Fig. 7). Fig. 7 ~~clearly~~ shows that the deglacial increase in atmospheric CO<sub>2</sub> has significant impacts on the Southern Ocean SST because the temperature trajectory is mostly proportional to CO<sub>2</sub> changes unless there are significant AMOC changes. Temperature changes associated with changes in AMOC are superimposed on Southern Ocean SSTs, in that an AMOC weakening ~~or strengthening~~ (blue ~~or red~~ circles) tends to induce a warming, and vice versa ~~or cooling, respectively~~. Even though the actual time series of AMOC in each model are very different, this result suggests that high southern latitude temperature changes can be decomposed into the effects of CO<sub>2</sub> and AMOC. The relative importance of CO<sub>2</sub> and AMOC are quantified in the following subsections.

### 3-4: Results of MLR model

The results of the MLR model indicate that the CO<sub>2</sub> coefficients range from 1.0 to 6.5°C for the total deglacial CO<sub>2</sub> changes (Table 4). All models have a negative coefficient of AMOC (–0.3 to –2.4°C), indicating a Southern Ocean SST increase associated with~~for~~ an AMOC weakening. The negative coefficient of AMOC in all models ~~results~~ suggest that an AMOC shutdown during HS1 has the potential to ~~increase temperature as CO<sub>2</sub> increases (which is able to explain about half of the total deglacial changes during HS1)~~ SST changes.

The regression against Southern Ocean 2-D SST fields indicates that the CO<sub>2</sub> coefficient is mostly positive over the Southern Ocean, ranging from ~0.5 °C in the Antarctic zone where sea ice is present until 11 ka, to 2–6 °C in the Southern Ocean north of the LGM winter sea ice edge (Fig. 8). The sensitivity to the AMOC is mostly negative in the Southern Ocean, and areas of high sensitivity overlap with those of CO<sub>2</sub>, suggesting sea ice modulates the areas sensitive to both CO<sub>2</sub> and AMOC changes.



### 3-5: Results of bipolar seesaw model

Table 5 summarises the results of the bipolar seesaw model. All models have positive CO<sub>2</sub> coefficients (2.0–6.0°C) and negative AMOC coefficients (–0.5 to –2.9°C), as in the MLR models. The time series simulated by the bipolar seesaw model are compared with actual SST changes and with MLR models in Fig. 9. The bipolar seesaw model succeeds in reproducing a gradual SST decrease as a result of an AMOC strengthening (e.g. gradual cooling in iTRACE and MIROC, 15–13 ka). This gradual cooling was not represented by the MLR model, which exhibits an immediate SST response to AMOC changes. The response time ranges from 100–700 years, with most models ranging from 500–700 years with the exception of LOVECLIM and iLOVECLIM (Table 5).

We note that [the values of the CO<sub>2</sub> sensitivity from the MLR and bipolar seesaw model may include gradual forcing from other greenhouse gases, ice sheets, and orbital forcing](#). In addition, a sharp cooling associated with freshwater in the Antarctic Ocean was not represented because both models, MLR and bipolar seesaw, do not consider meltwater in the Southern hemisphere (~14.5 ka of iTRACE and LOVECLIM, ~11.5 ka of MPI-ESM and iLOVECLIM)

### 3-6: Other Southern Ocean climate variables

We analyse AABW transport (minimum global meridional overturning streamfunction, at depths below 3000 m and 60°S–30°S) as an indicator of Southern Ocean meridional circulation, and 850 hPa zonal mean winds over the Southern Ocean (zonal mean winds averaged over 65°S–40°S). We focus on the onset of deglaciation (21–18 ka) and the initial significant increase in CO<sub>2</sub> (~HS1, 18–15 ka). The AABW (Fig. 10b) at the LGM ranges from 10 to 30 Sv among the six models and stays relatively constant between 21 and 18 ka. In the subsequent period (18–15 ka), iTRACE exhibits a significant decline in the AABW, in phase with Southern Ocean SST changes (Fig. 10d). LOVECLIM and MPI-ESM exhibit a gradual decline in AABW (~5 Sv), while three other models (MIROC, HadCM3, iLOVECLIM) exhibit a small reduction or a stable AABW. The zonal winds over the Southern Ocean do not change significantly between 21 and 18 ka, apart from MIROC and MPI-ESM, which exhibit a slight weakening (Fig. 10c). Between 18 and 15 ka, the zonal winds continue to decline in MIROC and MPI-ESM, and ~~also~~

start to decline in iTRACE and LOVECLIM. Little changes in zonal winds are simulated in iLOVECLIM, while HadCM3 exhibits a ~10% strengthening.

Subsurface ocean temperatures south of 60°S at depths of around 500 m (Fig. 10e) exhibit an increase during HS1 in 4 of the 6 simulations, with the largest warming (1.2 °C and 0.8 °C) simulated by the two simulations which exhibited the largest SST increase (iTRACE and MPI-ESM). During the ACR (15–13 ka), iTRACE and MIROC exhibit a gradual sub-surface temperature decrease while HadCM3 and MPI-ESM exhibit a continuous warming, as per the SST changes in the respective models. iLOVECLIM and LOVECLIM exhibit small changes (<0.5°C) in the total sub-surface temperature. Abrupt subsurface warming in iTRACE (~14 ka) and LOVECLIM (14.8–14.2 ka) coincide with Southern Ocean SST reduction, suggesting that this results from enhanced Southern Ocean stratification as a response to Southern Ocean meltwater input (Menviel et al., 2011; Lowry et al., 2018).

### **3-7: Additional freshwater experiments on HS1 SO warming in MIROC and HadCM3**

We additionally show two simulations run with the MIROC and HadCM3 models to assess the impact on southern high latitude climate of a significant AMOC decrease during HS1. In the MIROC simulations, the FWF during HS1 is increased to 0.1 Sv or 0.2 Sv between 18 and 15.5 ka (Figure 11a, red and orange lines) instead of 0.03 Sv in the standard simulation. This larger meltwater input further weakens the AMOC (Figure 11a) and leads to an additional 1 °C SST increase in the SO compared to the standard simulation. The 1 °C warming in response to AMOC reduction of ~5 Sv is significantly higher than results from the MLR and bipolar seesaw models. In the HadCM3 simulations, a North Atlantic freshwater flux of ~0.2 Sv during HS1 (similar to Trace-21ka A, Liu et al., 2009) significantly reduces the AMOC (Figure 11b blue lines), and induces an additional ~1 °C increase in Southern Ocean SST compared to the standard simulation. The results from the MIROC and HadCM3 sensitivity experiments show that the simulated warming during HS1 can be twice as strong with an AMOC shutdown compared to the standard simulation of each model. As in the LOVECLIM Heinrich stadial 4 simulation (Figure S2; Margari et al. 2020) the warming in the southern high latitude in response to AMOC strength is not necessarily linear, while MLR models assume a linear temperature response to the AMOC.

## 4. Discussion

### 4-1: Onset of deglacial warming

The climate forcing in the early deglaciation primarily comes from insolation due to obliquity and precession changes (Fig. 1a), which leads to an increase in spring to summer insolation south of 60 °S (Fig. S42). Ice core data suggest that the onset of deglacial warming at WDC was earlier than the increase in CO<sub>2</sub>, and this early deglacial warming has been suggested to result from an AMOC reduction (Shakun et al., 2012) or local insolation changes (WAIS project members, 2013). ~~Not all models show such warming and when a warming is simulated, However, simulated early warming it~~ is smaller than ~~estimated from~~ proxy records. Three models (MIROC, HadCM3, MPI-ESM) exhibit a small but significant warming (~ 0.5°C) between 21 and 18 ka (Fig. 4a) in both West and East Antarctica, as well as ~~in at the surface of the~~ Southern Ocean ~~SST~~, primarily in the Pacific sector (Fig. 4b) as suggested by proxy records (Moy et al., 2019; Sikes et al., 2019; Moros et al., 2021). ~~Although the~~ The amplitude of the early warming in these models is comparable to a previous modelling study (Timmermann et al., 2009), while the other models show a slight cooling (iTRACE ~~and LOVECLIM~~) or little change (LOVECLIM and iLOVECLIM).

The first explanation for the differences in the simulated temperature change between 21 and 18 ka is the ~~contrast in LGM climate states, and in particular, the extent of~~ Southern Ocean sea ice at LGM. MIROC, HadCM3 and MPI-ESM have less LGM summer sea ice than other ~~climate models, and the winter sea ice does not reach as far north: the northern margin of winter sea ice extent is located at ~60 °S in the Pacific sector, while it is at 50–55 °S in the other models (Fig. 4b bold lines). We note that these results for sea ice extent are within the range of reconstructions, as most recent proxy records combined with PMIP climate models estimated austral winter and summer sea ice extent to be around 60–55 °S and 65 °S, respectively (Lhardy et al., 2022; Green et al., 2022).~~ The smaller sea ice extent at the LGM, relative to other models, may lead to a high sensitivity to increased insolation allow the Southern Ocean to absorb increased incoming shortwave radiation during austral spring to summer, causing and induce significant warming with sea ice retreat (Timmermann et al., 2009; Roche et al., 2011). If the LGM Southern Ocean sea ice extent is extensive, the increase in insolation primarily south of 60 °S (Fig. S24) does not warm the Southern Ocean as much because of high sea ice albedo. Although the local insolation

changes are the likely cause of an early warming simulated in some of the models, the addition of freshwater could contribute to the AMOC weakening. For example, the consideration of an additional freshwater flux from the Fennoscandian ice sheet in the freshwater forcing prior to 18ka as included in MPI and, as suggested by Touccane et al. (2010), would weaken the AMOC and lead to a more pronounced warming in the southern high latitudes. The second explanation is the difference in the FWF. The three simulations that display an early deglacial warming include a FWF ( $\sim 0.02$  Sv) in the North Atlantic based on ICE-6G\_C (Fig. 2a). An early ice sheet discharge from the Fennoscandian ice sheet (Touccane et al., 2010) could have weakened the AMOC and contributed to the Southern Ocean warming.

Another model-data difference is the different early warming rates between West and East Antarctica. The data from WDC suggests there was significant warming in West Antarctica, while a less significant change in East Antarctica is suggested by EDC. In contrast, the models simulate similar warming rates in both West and East Antarctica (Fig. 4a), suggesting the models may underestimate the spatial heterogeneity in West and East Antarctic warming. This might be attributed to the Antarctic ice sheet history prescribed in the experiments, where both ICE-6G\_C and GLAC-1D have minor surface elevation changes at WDC in the early deglaciation (Fig. 1d). Buizert et al. (2021) used the MIROC and HadCM3 models and showed that the uncertainty in Antarctic ice sheet height affects the difference between LGM and PI temperatures because changes in surface elevation affect SAT ( $\sim 1$  °C per 100 m). This might suggest that the lower surface elevations at WDC, related to the ice sheet terminus retreat between 20–15 ka in the Amundsen Sea (Bentley et al. 2014), may have contributed to the early deglacial warming primarily in West Antarctica. The coarse resolution of the atmospheric models (2.5 to 5.6 degrees in the horizontal) may impact the warming contrast between EAIS and WAIS through an inherent smoothing of the surface topography of the Antarctic ice sheet and the associated impact on the atmospheric circulation. In addition, the relatively coarse resolution of the ocean models (1 to 3 degrees), may impact the AMOC sensitivity to iceberg and freshwater flux in the North Atlantic (Condon and Winsor 2012), or parameterizations of mesoscale processes in the Southern Ocean and their response to the deglaciation.

Uncertainty in the Antarctic ice sheet topography could also explain some model-data differences during the early Holocene, where simulations indicate more that an additional warming occurs after the

onset of the Holocene (Fig. 6). This is different from ice core data (Fig. 4) and global mean ocean temperature (including deep-sea temperature) estimated from noble gases in ice cores, which suggests that temperatures reach Holocene levels at the end of YD (Bereiter et al., 2018). The higher surface elevation of the Antarctic ice sheet at 11 ka compared to the present-day in the experimental design (Fig. 1e) may contribute to the simulated Holocene warming. [It would be valuable to assess the uncertainties from ice sheet reconstructions, as new reconstructions have been published \(e.g., Gowan et al., 2021\), and different LGM ice sheets can induce different AMOC variabilities \(Prange et al., 2023; Masoum et al., 2024\).](#)

#### 4-2: Rate of temperature changes

HS1 (~18–14.7 ka) exhibits significant warming in all models because of the CO<sub>2</sub> increase, with the total warming being dependent on the sensitivity of each model to CO<sub>2</sub> and to AMOC changes. iTRACE simulates the largest warming [during HS1 among six models, with an Antarctic SAT increase of 6–8°C and Southern Ocean SST of 4–5°C. While the Antarctic SAT matches, in both WDC and EDC, which is the closest to the warming rate from ice-core data, Southern Ocean SST is larger than the SST stack. Five models besides the iTRACE simulates a Southern Ocean SST change which compare well with the SST stack data, but these five models underestimate Antarctic SAT. This indicates that the different magnitudes of warming between Southern Ocean SST and Antarctic SAT are weakly simulated in models. among the six models. Estimates from the MLR and bipolar seesaw models indicate that both the increase in CO<sub>2</sub> during HS1 \(~40 ppm\) and the reduction in AMOC contributed to this warming. While iTRACE notably](#) exhibits the largest global mean SAT changes at the LGM (7.3 °C, compared to the six-model mean of 5.3 °C). ~~However,~~ the ECS of iTRACE (3.6 °C) is not the highest among the six models; [instead, MIROC4m has the highest ECS despite weaker deglacial warming](#) (Table 1). We examine the relationship between ECS and the LGM global mean SAT changes using multi-model PMIP3 and PMIP4 simulations (Fig. S43). We find a weak negative correlation (–0.06) between the ECS and global mean LGM SAT changes, and the [local SAT change anomalies](#) in the individual climate models can vary by about a factor of two even with the same ECS. A substantial asymmetry between warm and cold climates has been identified in previous studies because of the presence of continental ice sheets, ocean dynamics, and cloud feedback (Yoshimori et al., 2009; Zhu and Poulsen, 2021). Hence, [a good](#)

understanding ~~the mechanism and amplitude of cooling in the of the forcing and climate system feedback~~  
~~of the~~ LGM ~~simulations will contribute to a better understanding of multi-model differences in the climate~~  
~~is critical for evaluating the rate of deglacial warming during the last deglaciation.~~

The sensitivity to AMOC ranges ~~from between~~  $(-0.5 \text{ to } -2.9^\circ\text{C})$  ~~0.5–2.9 °C~~, based on the analysis  
using the thermal bipolar seesaw model (Table 5). A multi-model study comparing freshwater hosing  
experiments of 11 climate models (including LOVECLIM, MIROC, and HadCM3 used in this study)  
under LGM climate shows that ~~a majority most of~~ models exhibit warming in the Southern Ocean  
(Kageyama et al., 2013). However, the simulation length in their study is less than 420 years, as opposed  
to the estimated timescale in this study (~500–700 years), suggesting the need for longer simulations to  
~~estimate-evaluate~~ the extent of the climate response at high southern latitudes.

The MLR and thermal bipolar seesaw models in this study ~~may have include imply~~ ~~several~~  
~~assumptions a limited ability in disentangling the effects of CO<sub>2</sub> and AMOC or in considering non-linear~~  
~~responses. Firstly, as the gradual forcing is represented only by the CO<sub>2</sub> concentrations, they do not~~  
~~consider the effect from retreating ice sheets, meltwater flux in the Southern Ocean, or insolation changes~~  
~~explicitly. Other forcings besides CO<sub>2</sub> and AMOC, could be included in the CO<sub>2</sub> or AMOC coefficients,~~  
~~for instance, other gradual forcings have positive correlations with the CO<sub>2</sub> forcing. Antarctic and~~  
~~Northern Hemisphere ice sheet changes could impact Southern Ocean SST through deep-water formation.~~  
~~This may explain the CO<sub>2</sub> coefficients from the MLR and bipolar seesaw model that are higher than~~  
~~expected from ECS value. On the other hand, the AMOC sensitivity of the LOVECLIM model is low~~  
~~compared to the 1.5 °C Southern Ocean SST increase found in the simulation of Heinrich stadial 4~~  
~~(Margari et al. 2020, Fig. S4), and the CO<sub>2</sub> coefficient is quite high, potentially implying a poor~~  
~~separations of the two factors. For example, the AMOC sensitivity of the LOVECLIM model seems low~~  
~~compared to the 1.5 °C Southern Ocean SST increase found in the simulation of Heinrich stadial 4, in~~  
~~which the atmospheric CO<sub>2</sub> concentration was kept constant (Margari et al. 2020, Fig. S2). In addition, a~~  
~~MIROC simulation with a larger freshwater (0.1 Sv) during HS1 than in the standard deglaciation~~  
~~experiment exhibits a 0.5 °C higher Southern Ocean SST with a 3 Sv weaker AMOC (Fig. S3), indicating~~  
~~that the Southern warming in response to AMOC strength is nonlinear. Finally, the coefficients of CO<sub>2</sub>~~  
~~and AMOC are not necessarily constant in time, and other climate forcings derived from insolation and~~



~~continental ice sheets can impact temperature changes. Despite these limitations, these analyses can provide estimates of each model's deglacial sensitivity to CO<sub>2</sub> forcing and AMOC.~~

As shown here, the deglacial AMOC variations are quite different amongst the simulations. Only those which display an AMOC increase at the end of HS1 can capture a cooling trend corresponding to the ACR as suggested by ice-core data (iTRACE, LOVECLIM, MIROC). In comparison to previous transient simulations of the last deglaciation, the representation of the duration of the ACR has improved, as it was previously simulated as too short (Lowry et al., 2018). On the other hand, simulations that are forced with a large NH meltwater pulse consistent with ice sheet reconstructions do not simulate an ACR (Ivanovic et al., 2016; 2018; Kapsch et al., 2022; Bouttes et al., 2023). This so-called meltwater paradox (Ivanovic et al., 2018; Snoll et al., 2024) suggests a need for a better assessment of freshwater scenarios, and the potential sensitivity of climate models to freshwater forcing. We also note that the routing location of meltwater input (Roche et al., 2010; He et al., 2020) and the consideration of icebergs and meltwater discharge into the ocean (Schloesser et al., 2019; Love et al., 2021) may induce quite different AMOC changes. Regarding the BA, investigating the impacts of changing boundary conditions, typically those of ice sheets, GHGs and insolation, is necessary to reduce the gap between the climate responses and ice sheet reconstructions. Southern FWF can enhance the ACR, as found in iTRACE (~14.2 ka) and LOVECLIM (~14.7 ka), with a sharp cooling in Southern Ocean SST and Antarctic SAT primarily in WDC. This is caused by the intensified stratification in the Southern Ocean (Menviel et al., 2010; 2011), which induces significant warming in the subsurface and contributes to further mass loss from Antarctic ice sheets (Golledge et al., 2014). As ice core data does not exhibit such sharp cooling events as compared to climate model simulations (Fig. 3), this may provide some constraints on the extent and duration of FWF from the Antarctic ice sheet.

#### **4-3: Implications for climate system changes at high southern latitudes**

Reconstructions have suggested that changes in Southern Ocean circulation, probably driven by wind changes, were important for the modulation of Southern Ocean CO<sub>2</sub> outgassing during the deglaciation. Proxies~~In particular, marine sediment cores from the sub-Antarctic zone~~ suggest an enhanced opal flux during HS1, which could reflect increased upwelling in the Southern Ocean due to

changes in Southern Hemispheric westerlies (SHW) (Anderson et al., 2009), [and poleward shift of the SHW across the deglaciation \(Gray et al., 2023\)](#). ~~This is consistent with~~ Proxies also suggest decreasing deep and intermediate-depth Southern Ocean ventilation ages (Skinner et al., 2010, Burke et al., 2011), increasing intermediate-depth pH in the Southern Ocean during HS1 (Rae et al., 2018), ~~and a compilation of Southern Ocean  $\delta^{18}\text{O}$  records indicating a poleward shift of the SHW across the deglaciation (Gray et al., 2023)~~. ~~It has been suggested that a~~ Stronger or poleward-shifted SHW and/or enhanced AABW formation during HS1 would indeed enhance Southern Ocean  $\text{CO}_2$  outgassing and lead to an atmospheric  $\text{CO}_2$  increase ~~comparable to that from ice core estimates~~ (Menviel et al., 2014; Menviel et al., 2018). In contrast, [in the present study](#), most models show very little change or a gradual weakening in the SHW across the deglaciation, and there is little latitudinal migration of the SHW. Only the HadCM3 model displays a SHW strengthening [during HS1](#). However, additional studies should look in more details into potential changes in the location of the SHW in these simulations, as well as regional changes in SHW strength and their relation to other climatic variables (Rojas et al., 2009; Sime et al., 2013). In addition, no model exhibits an increase in AABW, which could contribute to the upwelling of carbon-rich water mass in the deep ocean and  $\text{CO}_2$  outgassing from the Southern Ocean. Instead, the deglaciation may have contributed to the long-term weakening in AABW by warming the Southern Ocean, enhancing sea ice melt, and decreasing surface salinity (Marson et al., 2016). While it has been suggested that larger Southern Ocean sea ice extent would lead to an atmospheric  $\text{CO}_2$  decrease at the LGM (Marzocchi et al., 2020, Stein et al., 2020), few models simulate significant changes in oceanic  $\text{CO}_2$  due to a Southern Ocean sea ice change (Gottschalk et al., 2019). These physical changes still need to be reconciled with processes put forward to explain the deglacial atmospheric  $\text{CO}_2$  changes by running coupled climate-carbon simulations.

Finally, we also find that changes in subsurface ocean temperature in the Southern Ocean, one of the critical factors impacting the retreat of the Antarctic ice sheet, display significant differences across the simulations. This could be related to different ECS or FWF in the Southern Ocean, and should also be investigated in future studies to quantify uncertainties in subsurface ocean temperature changes. Model-dependent subsurface ocean temperature change is one source of uncertainty in projecting future Antarctic ice sheet mass loss (Serrousi et al., 2020). In contrast to the present simulations of the last

616 deglaciation, which prescribe the Antarctic ice sheet history, climate variability occurring during the  
617 deglaciation can impact the Antarctic ice sheet, which can act as feedback to Southern Ocean climate via  
618 meltwater input from the Antarctic ice sheet (Menviel et al., 2010; Golledge et al., 2014; Clark et al.,  
619 2020). Hence, further coupled climate and ice sheet modelling studies are needed to improve our  
620 understanding of climatological and glaciological processes and to evaluate model performance under a  
621 warming climate and rising sea levels (Gomez et al., 2020).

## 622 5. Conclusion

623 In our multi-model analysis of transient deglacial experiments, ~~the most models simulate the onset~~  
624 ~~of the deglacial warming at high southern latitudes between 18 and 17 ka, in phase with the atmospheric~~  
625 ~~CO<sub>2</sub> increase. The early warming simulated increase in Antarctic SAT is weakly simulated or absent. The~~  
626 ~~multi-model difference some models~~ could be related to the smaller LGM sea ice extent, which may affect  
627 the sensitivity to insolation change, or to a slight reduction in the AMOC in response to small freshwater  
628 input from NH ice sheets. ~~The In addition, the different models do not exhibit significant differences in~~  
629 ~~the warming rates between West and East Antarctica, contrary to what is suggested by ice core records~~  
630 ~~are not reproduced by the transient simulations. In all models, a major~~ ~~The most rapid~~ warming occurs  
631 between 18 and 15 ka in response to increased CO<sub>2</sub> concentration, ~~The multi-model analysis and~~  
632 ~~sensitivity experiments further suggest that with the rate of warming being related to the climate~~  
633 ~~sensitivity of each model. The reduction in the AMOC reduction during HS1 associated with increased~~  
634 freshwater flux in the North Atlantic ~~as imposed in some models further contributes to the~~ ~~contributes to~~  
635 ~~a larger~~ warming, ~~in agreement with high southern latitude proxy records, even though no simulation~~  
636 ~~can reproduce both the amplitude of Southern Ocean SST and Antarctic SAT changes simultaneously.~~  
637 The ~~simulations bipolar seesaw model indicates all models have bipolar seesaw response, and further~~  
638 ~~suggest that~~ an abrupt AMOC increase at the end of HS1 is necessary to simulate the high southern latitude  
639 cooling corresponding to the ACR. ~~The amplitude and duration of the cooling is different between the~~  
640 ~~models because of the different North Atlantic freshwater scenarios, and the different amplitudes and~~  
641 ~~timescales of bipolar climate responses in each model.~~ The simulations do not exhibit significant changes  
642 in winds over the Southern Ocean or meridional circulation in the Southern Ocean, which could contribute  
643 to enhanced CO<sub>2</sub> outgassing from the Southern Ocean. This indicates the necessity for future climate

system modelling studies to quantify the sequence of [deglacial](#) climate changes and atmospheric CO<sub>2</sub> increase ~~during the last deglaciation~~.

## Acknowledgements:

[We thank the two anonymous referees for their valuable comments which have substantially improved our paper.](#) TO, AAO, TV and WLC acknowledge funding from JSPS Kakenhi 17H06104, 17H06323, and JPJSBP120213203. [TO was also supported by JPMXD0722680395 and JSPS kakenhi 24H00026.](#) We acknowledge discussions at PAGES-QUIGS T5–T0 workshops, supported by INQUA Terminations Five to Zero (T5–T0) Working Group (Project #2004). LM acknowledges funding from Australian Research Council (ARC) grants FT180100606 and SR200100008. UM and MK acknowledge funding by the German Federal Ministry of Education and Research as a Research for Sustainability Initiative through the PalMod project (grant nos. 01LP1915C, and 01LP1917B). The MLR analysis used scikit-learn library of Python 3.7. The figures were created using Generic Mapping Tool (GMT version 4 and 6).

## Data availability:

All model data supporting our findings will be archived at Zenodo. Original model data is upon request for authors from each modelling group.

## Code availability:

The bipolar seesaw model and the MLR model used in this study can be shared upon request.

## Author contribution:

TO, LM, and AAO conceived the study. TO, LM, TV, BS analysed the data. TO, LM, AAO, TV, RI, and BS wrote the manuscript with input from all co-authors.

## Competing interests:

Laurie Menviel is a member of the editorial board of Climate of the Past, but otherwise all authors declare that they have no conflict of interest.

## References:

Name	Climate model name	ECS [K]	Global mean	
			LGM SAT anomaly [K]	References
iTRACE	iCESM1.3	3.6	7.3	Tierney et al., (2020)
LOVECLIM	LOVECLIM	2.8	4.2	McDougall et al., (2020), <a href="#">Goosse et al., (2010)</a>
MIROC	MIROC4m	3.9	4.5	Chan and Abe-Ouchi, (2020)
HadCM3	HadCM3B	2.7	6.1	Kageyama et al., (2021)
MPI-ESM	MPI-ESM-CR P2		6.1	
iLOVECLIM	iLOVECLIM	2.0	3.5	

**Table 1:** Summary of climate models analysed in this study. Note that the ECS for MPI-ESM (model version MPI-ESM-CR P2) has not been calculated.

Name	Freshwater scheme	GHGs	Ice sheets	References for deglaciation experiments
iTRACE	TraCE-like	PMIP4	ICE-6G_C	He et al., 2019; 2021
LOVECLIM	TraCE-like	Kohler et al., 2017	ICE-5G	Menviel et al., 2011
MIROC	ICE-6G_C with adjustment	PMIP4	ICE-5G (LGM fix)	Obase and Abe-Ouchi 2019; Obase et al., 2021
HadCM3	ICE-6G_C	PMIP4	Ice-6G_C	Ivanovic et al., 2018; Snoll et al., 2022
MPI-ESM	ICE-6G_C	Kohler et al., 2017	Ice-6G_c	Kapsch et al., 2022
iLOVECLIM	ICE-6G_C	PMIP4	Ice-6G_c	Bouttes et al., 2023

**Table 2:** Summary of the experimental design used in the transient deglacial simulations.

676

Parameter [unit]	Range
CO <sub>2</sub> coefficient $\alpha$ [K/83 ppm]	1.0–7.0, every 0.2
AMOC coefficient $\beta$ [K/(normalised AMOC)]	0.0–3.0, every 0.1
Response timescale $\tau$ [year]	100–1000, every 100

**Table 3:** Parameter ranges in the thermal bipolar seesaw model.

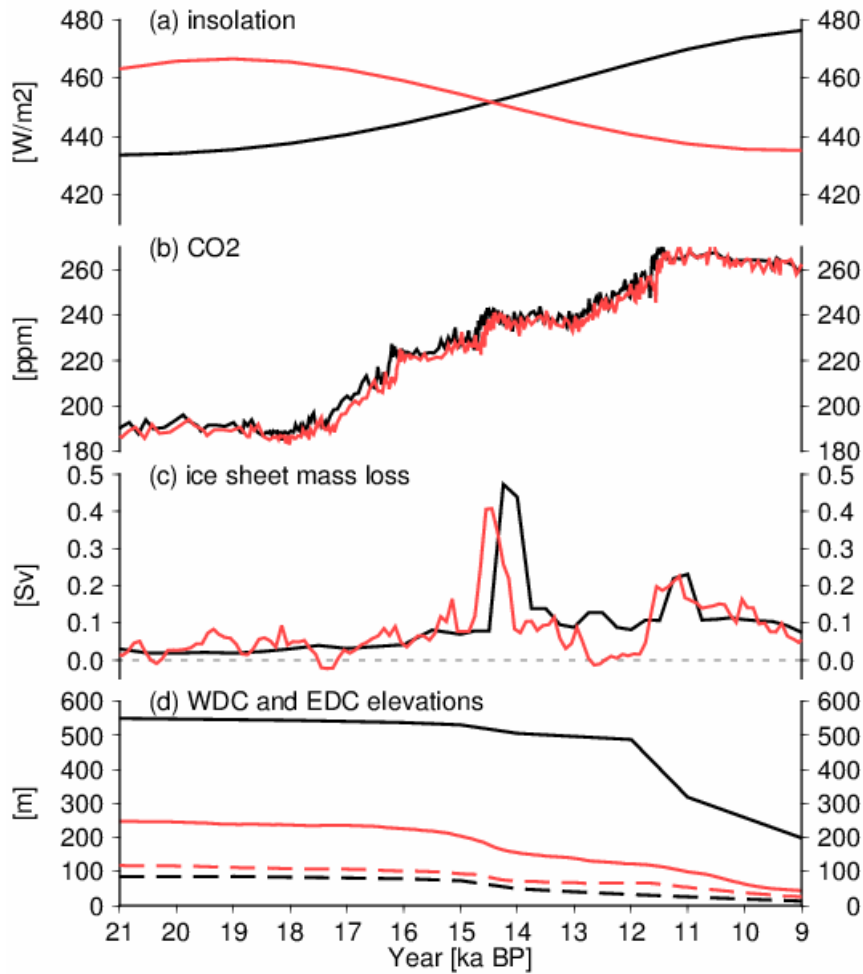
	CO <sub>2</sub> coefficient [K/83 ppm]	AMOC coefficient [K/(normalised AMOC)]	Coefficient of Determination
iTRACE	6.5	−2.4	0.90
LOVECLIM	4.1	−0.4	0.91
MIROC	1.4	−0.5	0.81
HadCM3	3.3	−1.4	0.95
MPI-ESM	3.1	−1.2	0.90
iLOVECLIM	1.0	−1.4	0.56

677 **Table 4:** Results of the MLR model for Southern Ocean SST.

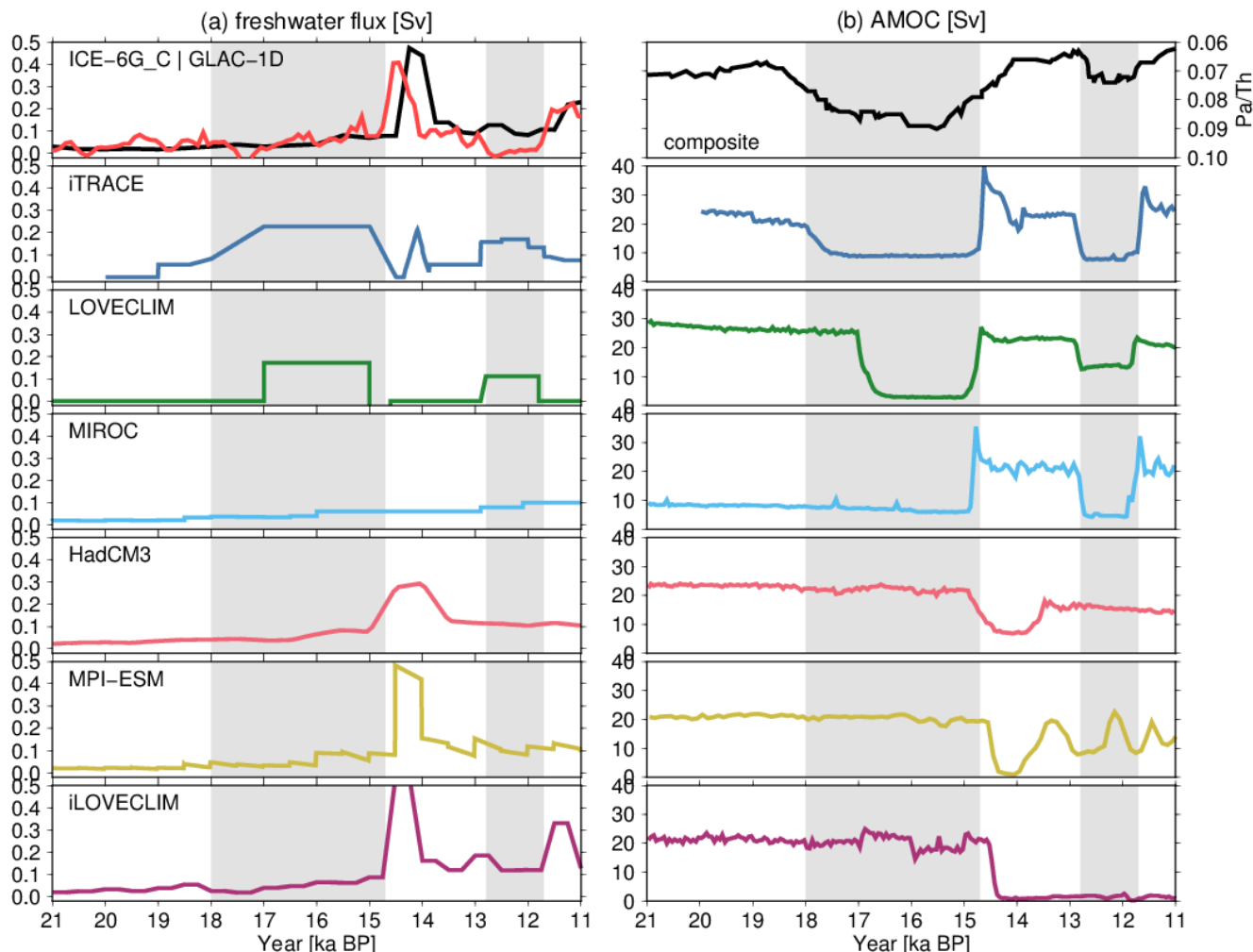
	CO <sub>2</sub> coefficient [K/83 ppm]	AMOC coefficient [K/(normalised AMOC)]	Response timescale [year]	<a href="#">Coefficient of determination</a>
iTRACE	6.0	−2.9	500	<a href="#">0.97</a>
LOVECLIM	4.4	−0.6	300	<a href="#">0.94</a>
MIROC	2.4	−0.9	600	<a href="#">0.97</a>
HadCM3	4.8	−1.3	700	<a href="#">0.99</a>
MPI-ESM	3.4	−1.4	500	<a href="#">0.95</a>
iLOVECLIM	2.0	−0.8	100	<a href="#">0.54</a>

678 **Table 5:** Results of the bipolar seesaw model for Southern Ocean SST

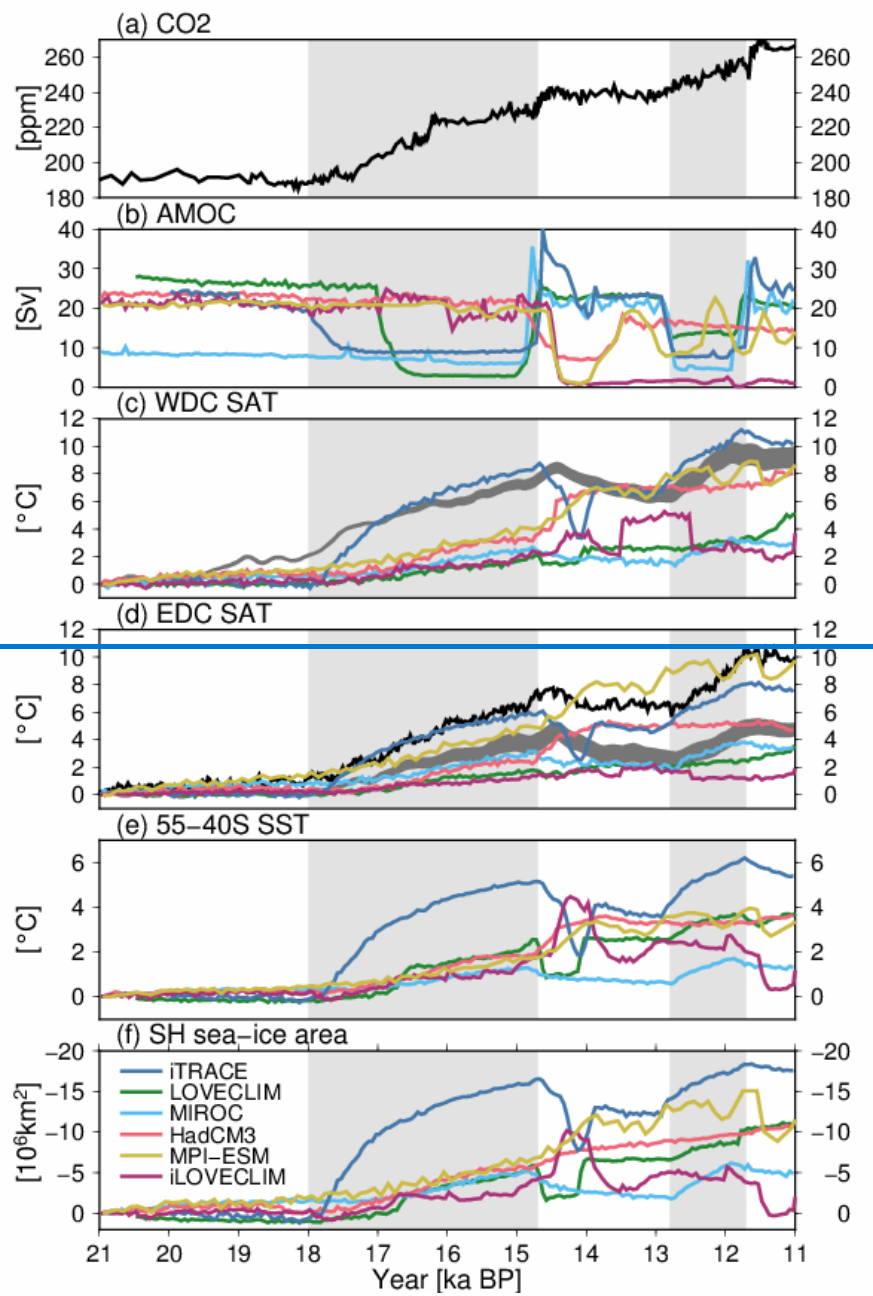




**Figure 1:** Forcing of the last deglaciation. (a) Insolation. Black: 65°N July, red: 65°S January based on Berger (1978), (b) CO<sub>2</sub>. Black: Bereiter et al., (2015), red: Kohler et al., (2017), (c) FWF in the NH from ICE-6G\_C (black lines) and GLAC-1D (red lines), (d-e) Elevation change at WDC (bold lines) and EDC (dashed lines) from ICE-6G\_C and GLAC-1D.



**Figure 2:** (a) Freshwater forcing (total value in the NH) and (b) simulated [AMOC](#) time series ~~of AMOC~~. The top panels indicate the freshwater flux from ice sheet reconstructions (black indicates ICE-6G\_C and red indicates GLAC-1D) and composite  $^{231}\text{Pa}/^{230}\text{Th}$  in the North Atlantic, retrieved from Ng et al., (2018). The grey shading indicates HS1 (18–14.7ka) and the YD (12.8–11.7ka), respectively, and the period in between corresponds to the BA (14.7–12.8 ka). .



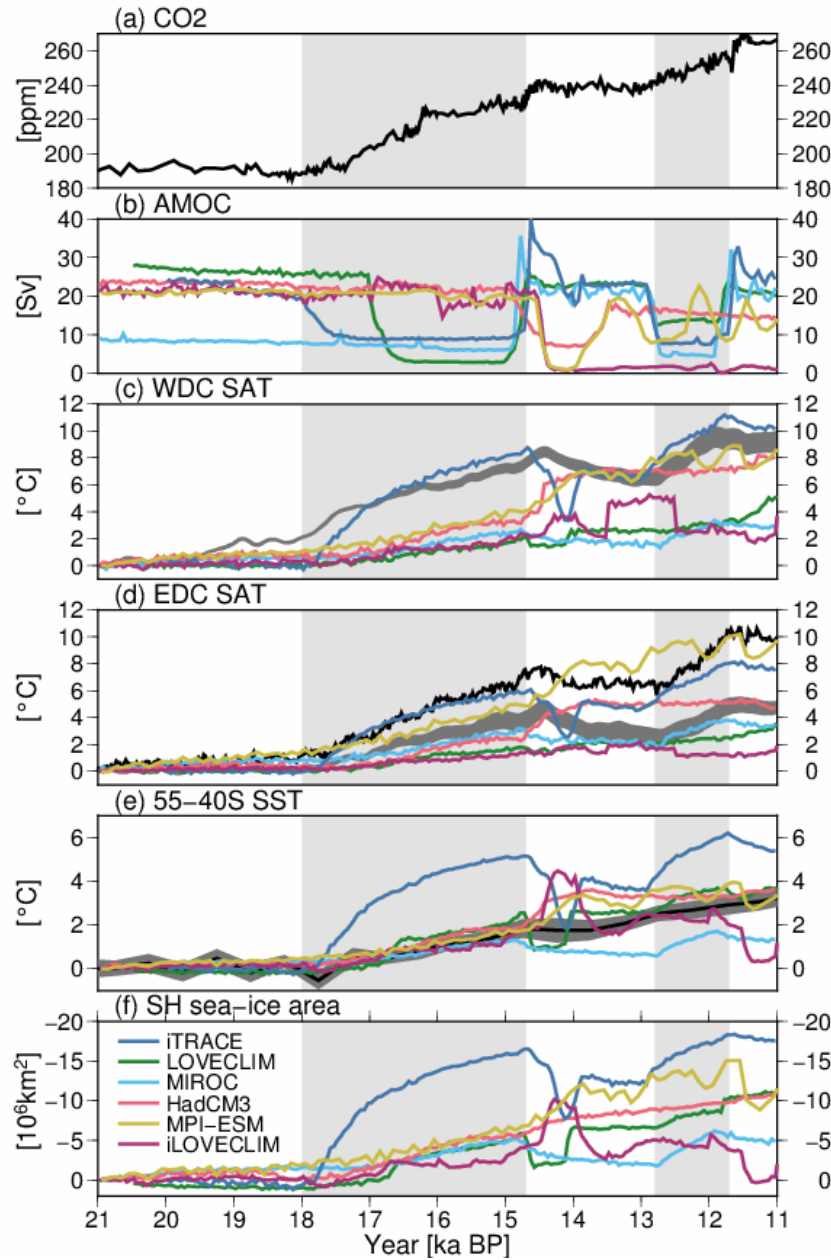


**Figure 3:** Time series of (a) atmospheric CO<sub>2</sub> (Bereiter et al., 2015) and (b) simulated AMOC, (c–d) SAT at WDC and EDC, (e) Southern Ocean SST, (f) Southern Ocean sea ice area in the transient simulations. The SAT, SST and sea ice area indicate changes since the LGM. The grey lines in (c–d) represent reconstructions from Buizert et al., (2013), and the black line in (d) represents reconstructions from Parrenin et al., (2013). [The black lines and grey shades in \(e\) indicate the Southern Ocean SST stack and its standard error, respectively, as derived by Anderson et al., \(2020\).](#)

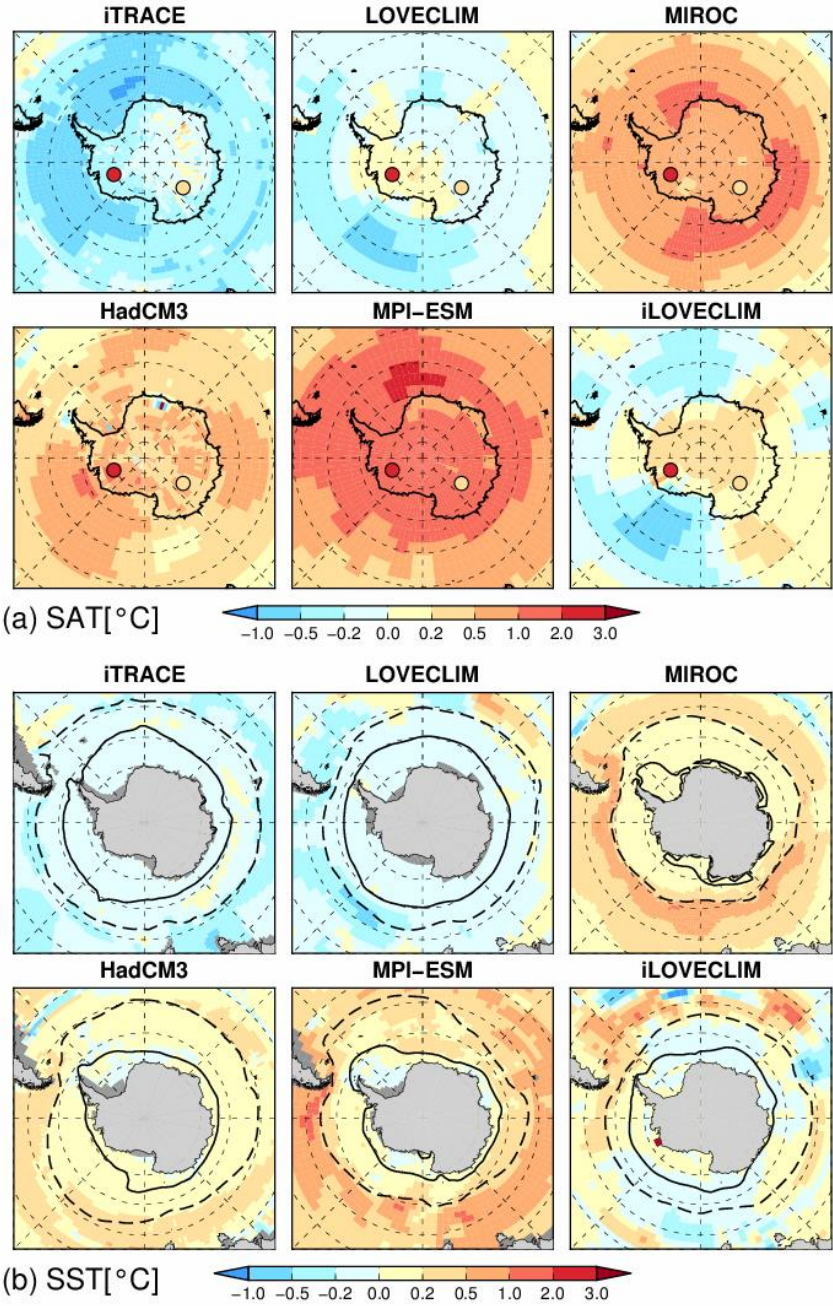
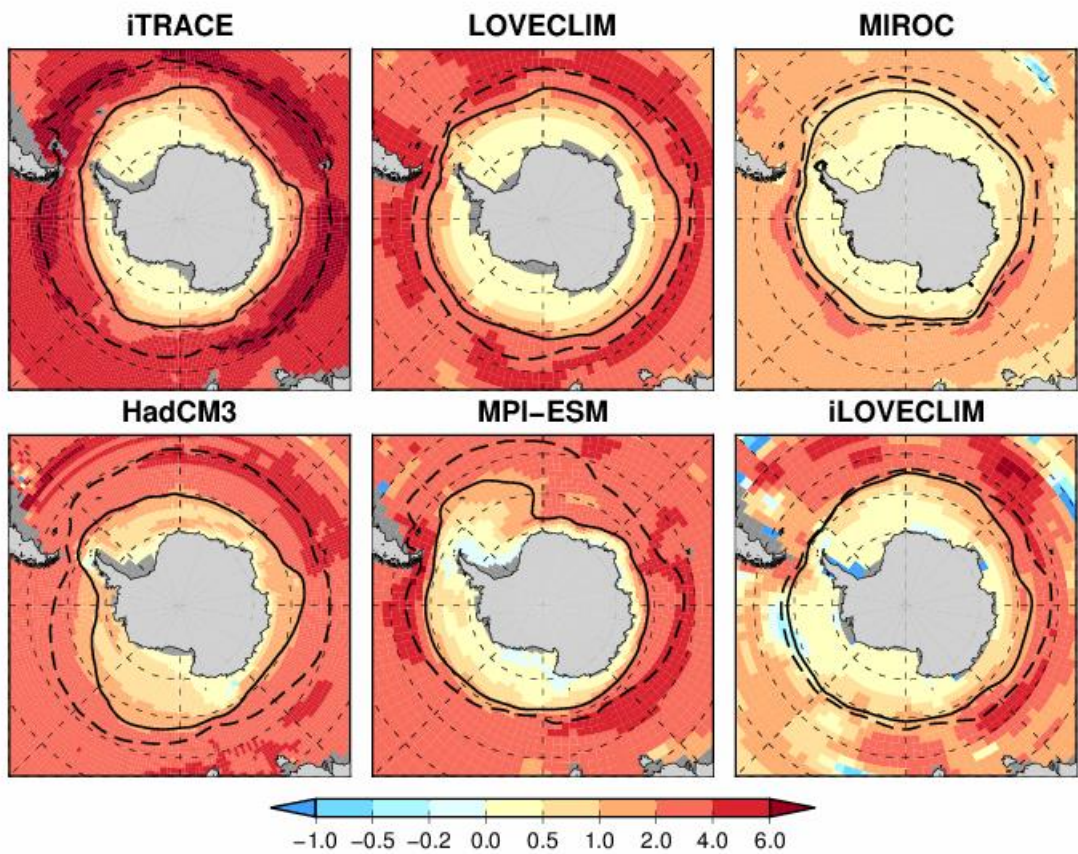


**Figure 4:** (a) SAT and (b) SST anomalies at 18 ka compared to the LGM. The coloured circles in (a) represent 18 ka-LGM [warming-SAT change](#) based on ice core data (Parrenin et al., 2013), and the bold



702 and dashed lines in (b) represent LGM austral summer and winter sea ice extent (85 and 15% annual-  
703 mean sea ice concentration), [respectively](#).



704  
705 **Figure 5:** SST anomalies at 11 ka compared to the LGM. The bold and dashed lines indicate LGM and  
706 11 ka sea ice extent (15% sea ice concentration), respectively.



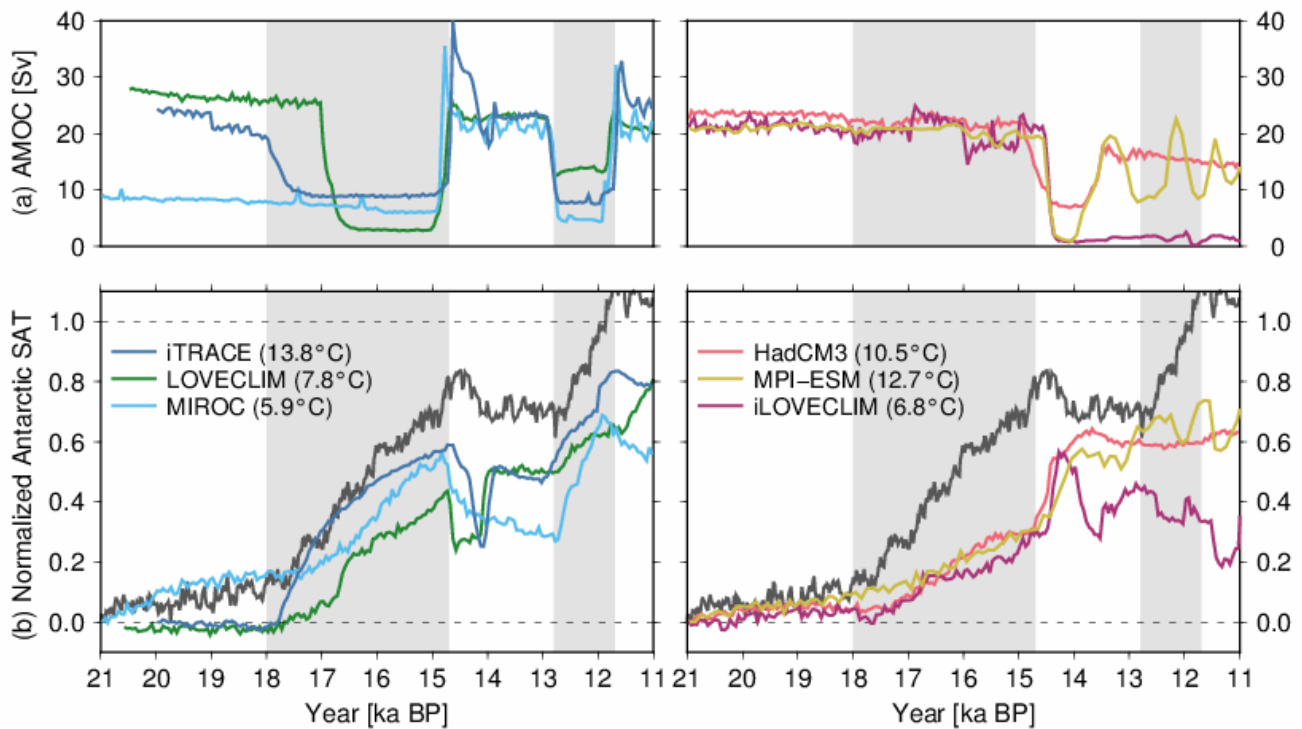


**Figure 6:** AMOC and normalised Antarctic SAT, with respect to the difference between PI and LGM. The actual PI and LGM differences are indicated in parentheses. The left panels show three simulations with weak AMOC during HS1, and the right show strong AMOC during HS1, respectively. The grey line in (b) is normalised Antarctic SAT from EDC based on Parrenin et al., 2013.

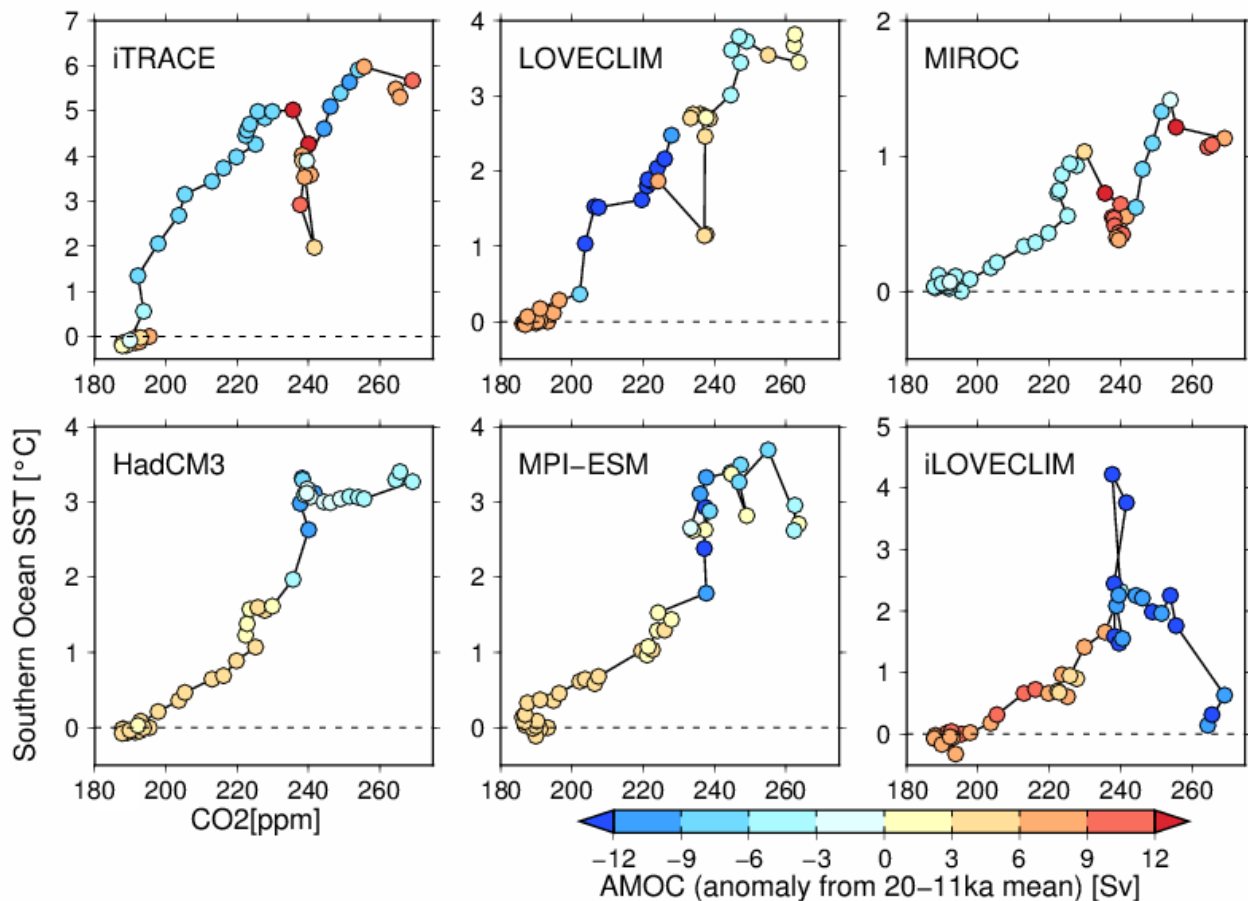


**Figure 7:** Relationship between Southern Ocean SST (vertical axis, change since LGM), CO<sub>2</sub> (horizontal axis) and AMOC strength anomaly from the mean strength between 20–11 ka (colours). The trajectory of the deglacial CO<sub>2</sub> forcing (CO<sub>2</sub>), simulated SST changes and AMOC are plotted with circles at 200-year intervals. Note that the vertical axes are different between models to represent the total deglacial warming.

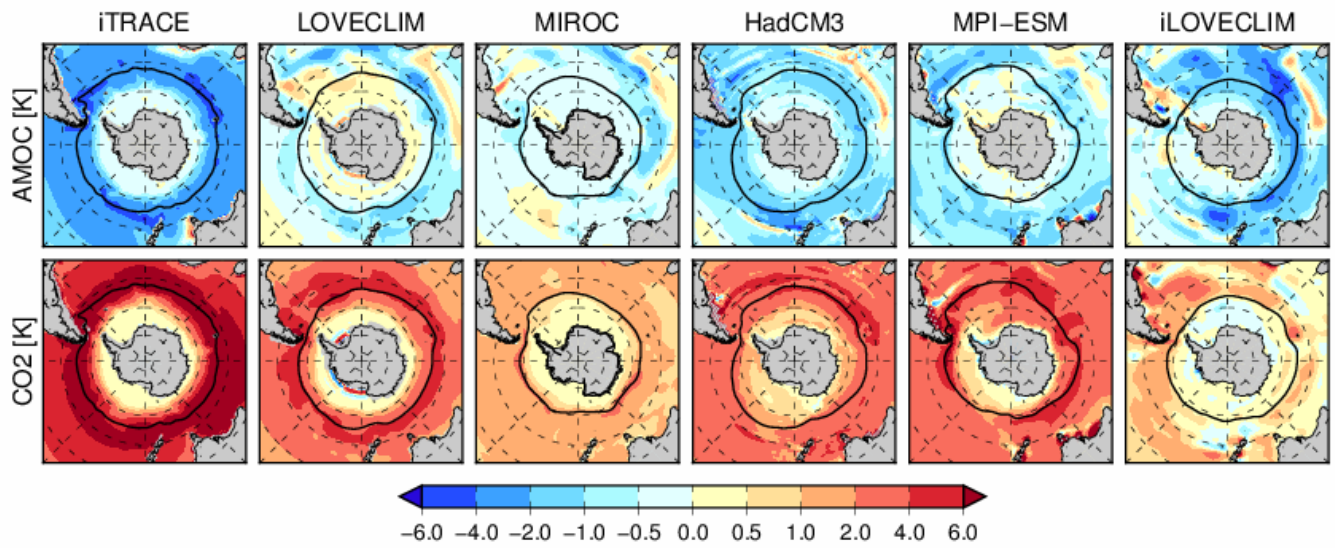


**Figure 8:** Results of the MLR model for 2-D SST maps. Top: AMOC coefficients. Bottom: CO<sub>2</sub> coefficients. The black lines represent LGM sea ice edges.

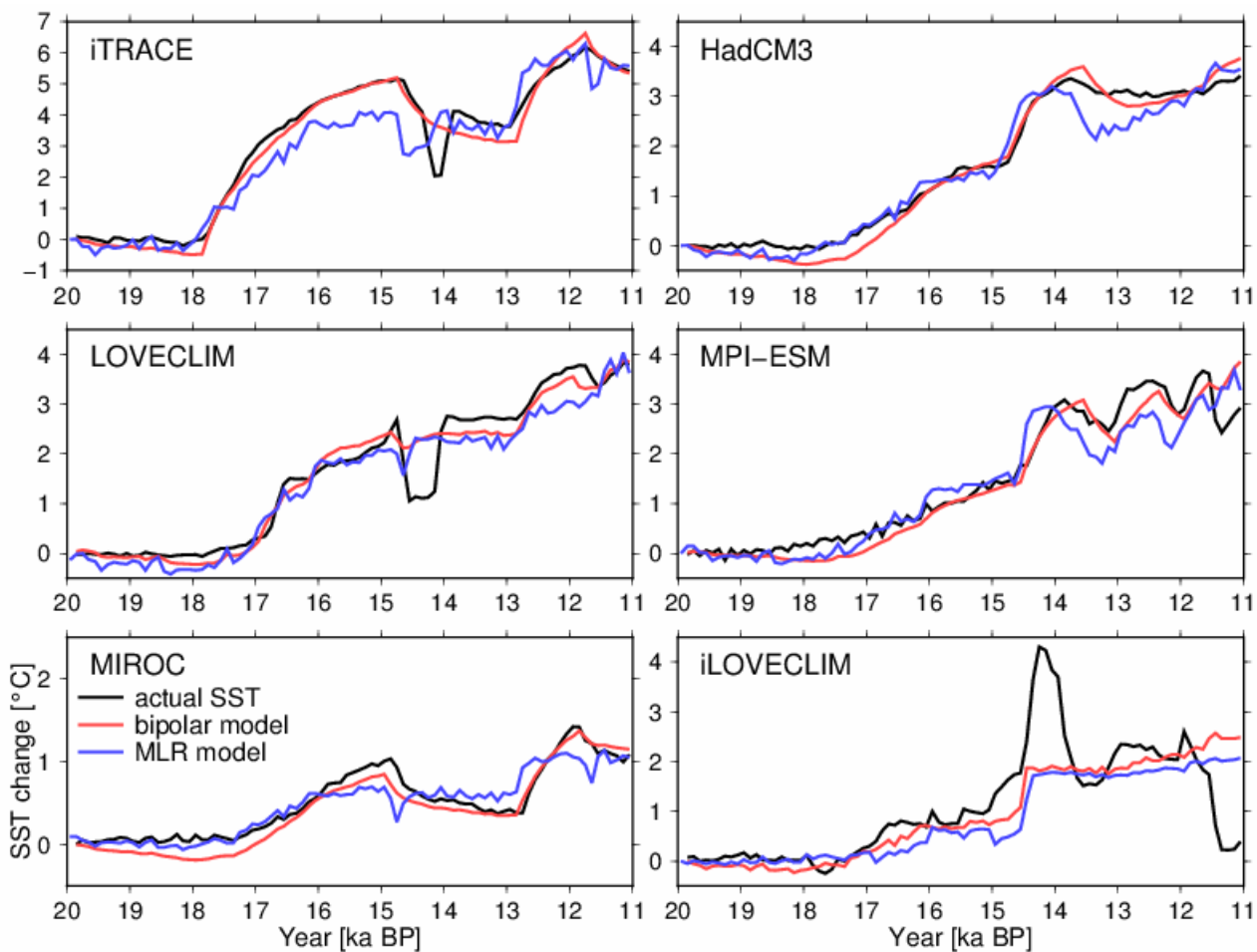


**Figure 9:** Results of the MLR model and bipolar seesaw model for Southern Ocean SST. The black lines represent the actual SST change (anomaly from 20 ka). The blue and red lines represent the results of MLR and bipolar seesaw models, respectively.

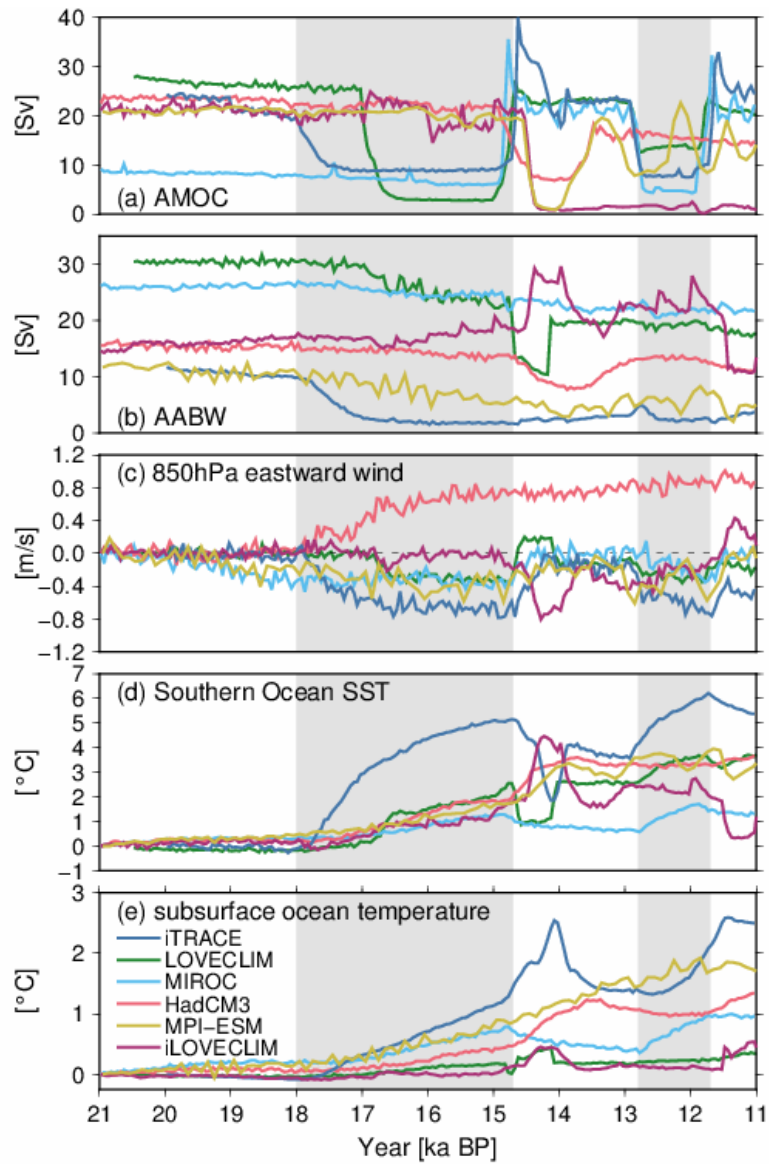


**Figure 10:** Time series of simulated (a) AMOC, (b) AABW, (c) 850hPa winds over the Southern Ocean (65–40°S), (d) Southern Ocean SST, and (e) subsurface ocean temperature south of 60°S (at depths 400–666-m).

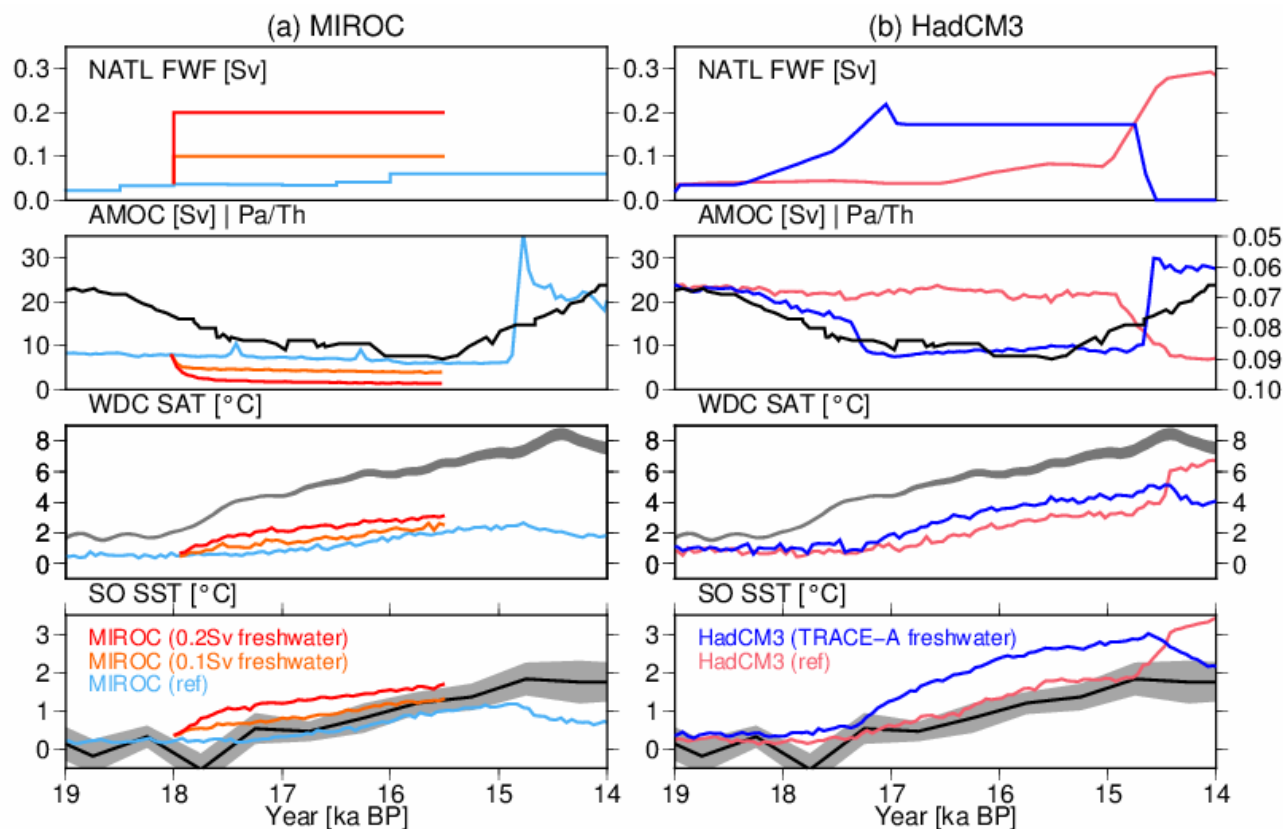


**Figure 11:** Results from transient deglaciation experiments performed with (a) MIROC and (b) HadCM3. The black lines in each panel represent the same proxy data as in Figure 3 (Parrenin et al., 2013; Buizert et al., 2021; Anderson et al., 2020). In two MIROC sensitivity experiments, a larger amount of freshwater flux (0.1 or 0.2 Sv) is added into the North Atlantic (50–70°N) during 18–15.5 ka compared to the standard MIROC experiment (light blue lines). In the TRACE-A HadCM3 sensitivity experiment (blue lines), a larger freshwater flux is added in the North Atlantic following the Trace-21ka simulation (Liu et al., 2009), while the pink lines in (b) represent the HadCM3 simulation used in Snoll et al. (2022).

Supplemental Figures:

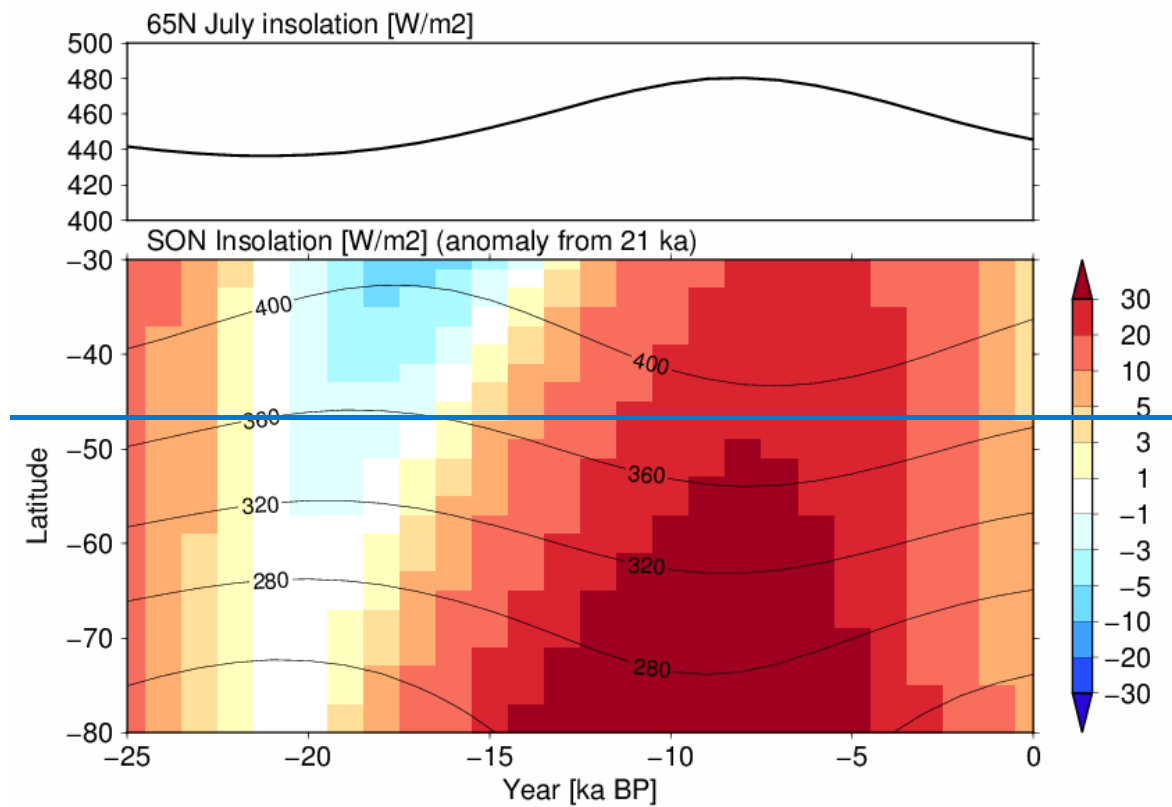


**Figure S1:** (top) 65°N July insolation, (bottom) austral spring to summer (September to November) insolation. The contours indicate absolute values of the mean insolation, and colours indicate anomaly from 21 ka.



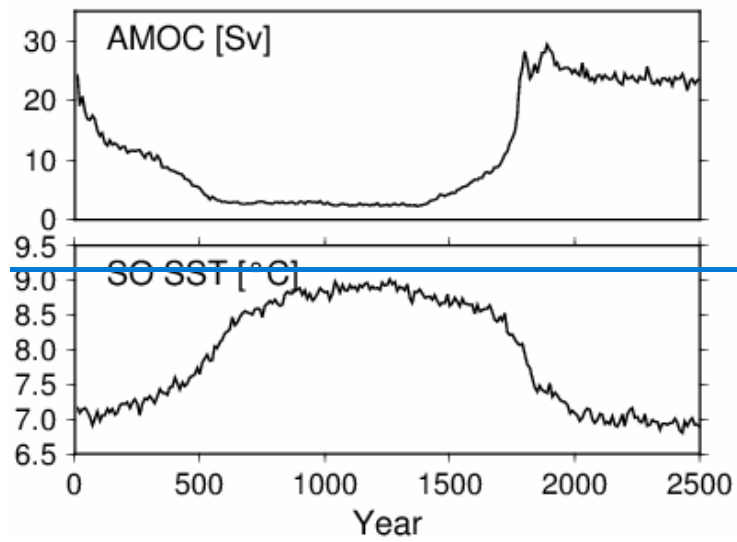


**Figure S2:** Results from a North Atlantic meltwater experiment performed with LOVECLIM under 40ka boundary conditions and with an atmospheric CO<sub>2</sub> concentration fixed at 195 ppm (Margari et al., 2020). Freshwater is added into the North Atlantic (50–60°N). The freshwater flux is increased linearly to 0.2 Sv during the first 400 years, decreased linearly to zero during the next 400 years, and remains at zero thereafter.

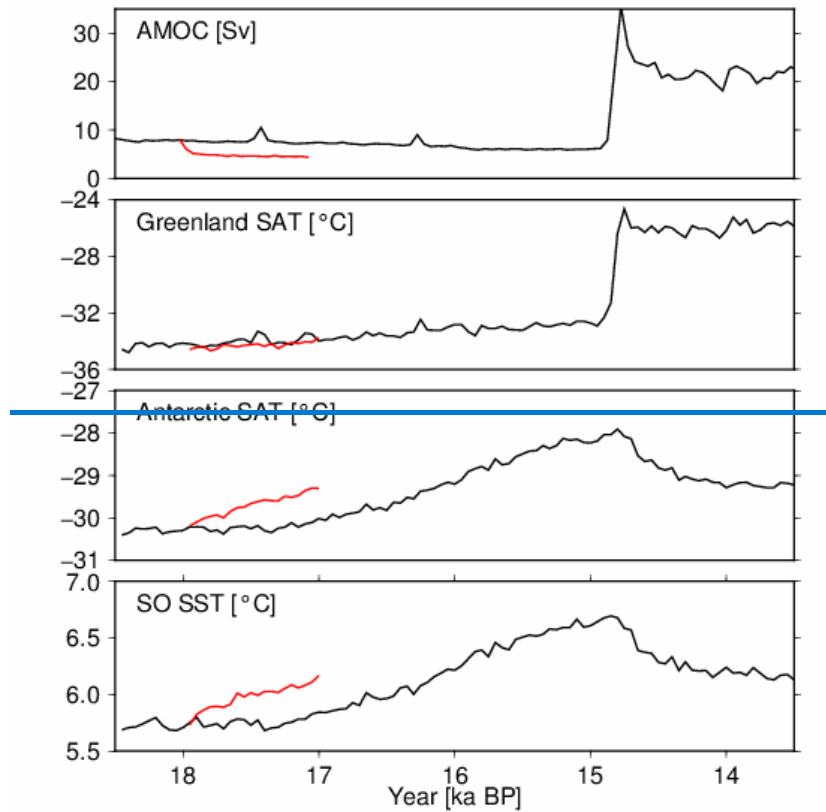


**Figure S3:** Results from a deglaciation experiment with MIROC (red lines), where a uniform freshwater flux of 0.1 Sv is added into the North Atlantic (50–70°N) during 18–17 ka. Black lines represent the standard deglaciation experiment.

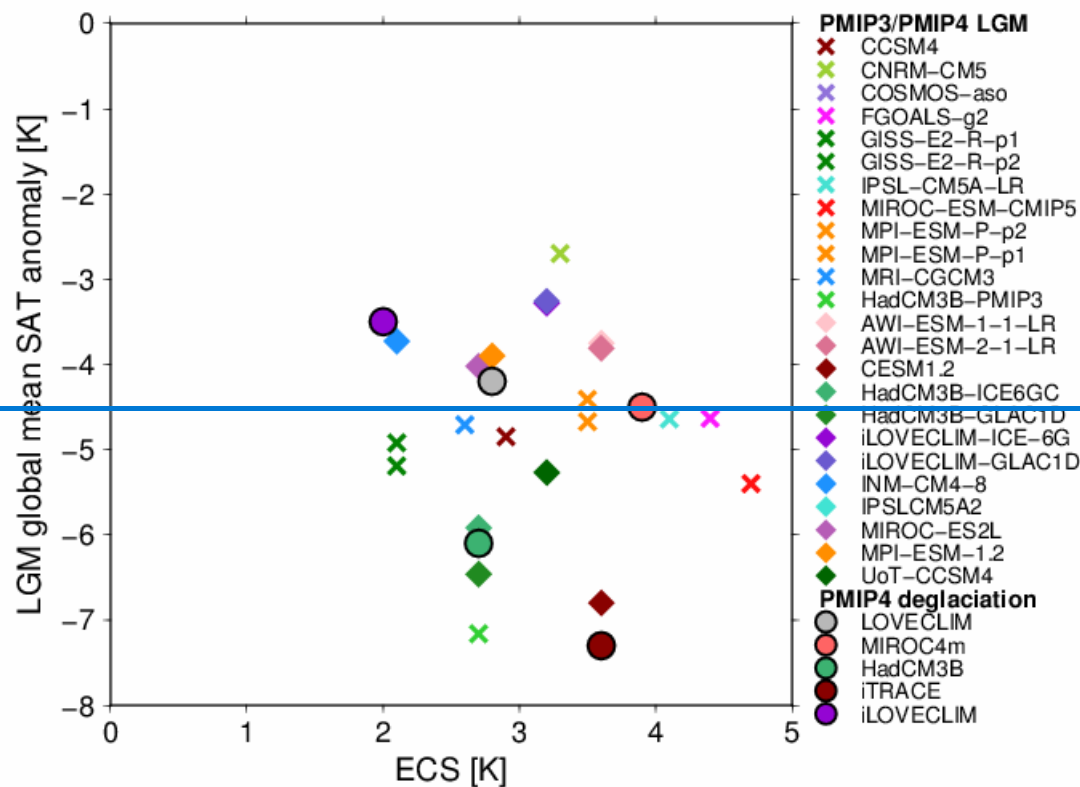


**Figure S4:** Relationship between the equilibrium climate sensitivity (ECS) and global mean temperature changes for the LGM. The circles indicate PMIP4 deglaciation (this study), and crosses and diamonds indicate LGM simulations from PMIP3 and PMIP4 (summarised in Kageyama et al., 2021), respectively.

## References

1. Abe-Ouchi, A., Saito, F., Kawamura, K., Raymo, M. E., Okuno, J., Takahashi, K., and Blatter, H.: Insolation-driven 100,000-year glacial cycles and hysteresis of ice-sheet volume. *Nature* 500, 190–193, doi: 10.1038/nature12374, 2013
2. Anderson, B. E., & Burckle, L. H.: Rise in Atmospheric CO<sub>2</sub>. *Science*, 323 (March), 1443–1448, 2009
3. Anderson, H. J., Pedro, J. B., Bostock, H. C., Chase, Z., and Noble, T. L.: Compiled Southern Ocean sea surface temperatures correlate with Antarctic Isotope Maxima, *Quaternary Science Reviews*, 255, 106821, <https://doi.org/10.1016/j.quascirev.2021.106821>, 2021.

- ~~2.4.~~ [Anderson, Harris J; Pedro, Joel B; Bostock, Helen C; Chase, Zanna; Noble, Taryn L \(2020\): Southern Ocean Sea Surface Temperature Anomaly Stacks \[dataset\]. PANGAEA, <https://doi.org/10.1594/PANGAEA.912158>](#)
- ~~3.5.~~ [Annan, J. D., Hargreaves, J. C., and Mauritsen, T.: A new global surface temperature reconstruction for the Last Glacial Maximum, \*Clim. Past\*, 18, 1883–1896, <https://doi.org/10.5194/cp-18-1883-2022>, 2022.](#)
- ~~4.6.~~ [Bentley, M. J., Ocofaigh, C., Anderson, J. B., Conway, H., Davies, B., Graham, A. G. C., Hillenbrand, C. D., Hodgson, D. A., Jamieson, S. S. R., Larter, R. D., Mackintosh, A., Smith, J. A., Verleyen, E., Ackert, R. P., Bart, P. J., Berg, S., Brunstein, D., Canals, M., Colhoun, E. A., Crosta, X., Dickens, W. A., Domack, E., Dowdeswell, J. A., Dunbar, R., Ehrmann, W., Evans, J., Favier, V., Fink, D., Fogwill, C. J., Glasser, N. F., Gohl, K., Golledge, N. R., Goodwin, I., Gore, D. B., Greenwood, S. L., Hall, B. L., Hall, K., Hedding, D. W., Hein, A. S., Hocking, E. P., Jakobsson, M., Johnson, J. S., Jomelli, V., Jones, R. S., Klages, J. P., Kristoffersen, Y., Kuhn, G., Leventer, A., Licht, K., Lilly, K., Lindow, J., Livingstone, S. J., Massé, G., McGlone, M. S., McKay, R. M., Melles, M., Miura, H., Mulvaney, R., Nel, W., Nitsche, F. O., O'Brien, P. E., Post, A. L., Roberts, S. J., Saunders, K. M., Selkirk, P. M., Simms, A. R., Spiegel, C., Stollendorf, T. D., Sugden, D. E., van der Putten, N., van Ommen, T., Verfaillie, D., Vyverman, W., Wagner, B., White, D. A., Witus, A. E., and Zwart, D.: A community-based geological reconstruction of Antarctic Ice Sheet deglaciation since the Last Glacial Maximum, \*Quaternary Sci. Rev.\*, 100, 1–9, <https://doi.org/10.1016/j.quascirev.2014.06.025>, 2014.](#)
- ~~5.7.~~ [Berger, A.: Long-Term Variations of Daily Insolation and Quaternary Climatic Changes, \*J. Atmos. Sci.\*, 35, 2362–2367, doi:10.1175/1520-0469\(1978\)035<2362:LTVODI>2.0.CO;2, 1978.](#)
- ~~6.8.~~ [Bereiter, B., Eggleston, S., Schmitt, J., Nehrbass-Ahles, C., Stocker, T. F., Fischer, H., Kipfstuhl, S., and Chappellaz, J.: Revision of the EPICA Dome C CO<sub>2</sub> record from 800 to 600 kyr before present, \*Geophys. Res. Lett.\*, 42, 542–549, \[10.1002/2014GL061957\]\(https://doi.org/10.1002/2014GL061957\), 2015.](#)
- ~~7.9.~~ [Bereiter, B., Shackleton, S., Baggenstos, D., Kawamura, K., and Severinghaus, J.: Mean global ocean temperatures during the last glacial transition. \*Nature\*, 553\(7686\), 39–44. <https://doi.org/10.1038/nature25152>, 2018.](#)

800 ~~8~~10. Bethke, I., Li, C., and Nisancioglu, K. H.: Can we use ice sheet reconstructions to constrain  
801 meltwater for deglacial simulations? *Paleoceanography*, 27 (November 2011), 1–17.  
802 doi:10.1029/2011PA002258, 2012

803 ~~9~~11. Böhm, E., Lippold, J., Gutjahr, M., Frank, M., Blaser, P., Antz, B., Fohlmeister, J., Frank, N.,  
804 Andersen, M. B. and Deininger, M.: Strong and deep Atlantic meridional overturning circulation  
805 during the last glacial cycle. *Nature*, 517(7534), 73–76. <https://doi.org/10.1038/nature14059>, 2015.

806 ~~10~~12. Bouttes, N., Roche, D. M., and Paillard, D.: Systematic study of the impact of fresh water fluxes  
807 on the glacial carbon cycle, *Clim. Past*, 8, 589–607, <https://doi.org/10.5194/cp-8-589-2012>, 2012.

808 ~~11~~13. Bouttes, N., Lhardy, F., Quiquet, A., Paillard, D., Goosse, H., and Roche, D. M.: Deglacial climate  
809 changes as forced by different ice sheet reconstructions, *Clim. Past*, 19, 1027–1042,  
810 <https://doi.org/10.5194/cp-19-1027-2023>, 2023.

811 ~~12~~14. Buizert, C., Gkinis, V., Severinghaus, J. P., He, F., Lecavalier, B. S., Kindler, P., Leuenberger,  
812 M., Carlson, A. E., Vinther, B., Masson-Delmotte, V., White, J. W. C., Liu, Z., Otto-Bliesner, B.,  
813 and Brook, E. J.: Greenland temperature response to climate forcing during the last deglaciation,  
814 *Science*, 345, 1177–1180, [10.1126/science.1254961](https://doi.org/10.1126/science.1254961), 2014.

815 ~~13~~15. Buizert, C., Fudge, T. J., Roberts, W. H., Steig, E. J., Sherriff-Tadano, S., Ritz, C., Lefebvre, E.,  
816 Edwards, J., Kawamura, K., Oyabu, I., Motoyama, H. Kahle, E. C., Jones, T. R., Abe-ouchi, A.,  
817 Obase, T., Martin, C., Corr, H., Severinghaus, J. P., Beaudette, R. Epifanio, J. A., Brook, E. J., Martin,  
818 K., Aoki, S., Nakazawa, T., Sowers, T. A., Alley, R. B., Ahn, J., Sigl, M., Severi, M., Dunbar, N. W.,  
819 Svensson, A., Fegyveresi, J. M., He, C., Liu, Z., Zhu, J., Otto-bliesner, B. L., Lipenkov, V. Y.,  
820 Kageyama, M., and Schwander, J.: Antarctic surface temperature and elevation during the Last  
821 Glacial Maximum, *Science* 372(6546), 1097-1101, doi: [10.1126/science.abd2897](https://doi.org/10.1126/science.abd2897), 2021

822 ~~14~~16. Burke, A. and Robinson, L. F.: The Southern Ocean’s Role in Carbon Exchange During the Last  
823 Deglaciation, *Science*, 135, 6068, 557-561. <https://doi.org/10.1126/science.1208163>, 2011

824 ~~15~~17. Capron, E., Landais, A., Chappellaz, J., Schilt, A., Buiron, D., Dahl-Jensen, D., Johnsen, S. J.,  
825 Jouzel, J., Lemieux-Dudon, B., Loulergue, L., Leuenberger, M., Masson-Delmotte, V., Meyer, H.,  
826 Oerter, H., and Stenni, B.: Millennial and sub-millennial scale climatic variations recorded in polar

ice cores over the last glacial period, *Clim. Past*, 6, 345–365, <https://doi.org/10.5194/cp-6-345-2010>, 2010.

~~16~~18. Chan, W.-L. and Abe-Ouchi, A.: Pliocene Model Intercomparison Project (PlioMIP2) simulations using the Model for Interdisciplinary Research on Climate (MIROC4m), *Clim. Past*, 16, 1523–1545, <https://doi.org/10.5194/cp-16-1523-2020>, 2020.

~~17~~19. Clark, P. U., He, F., Golledge, N. R., Mitrovica, J. X., Dutton, A., Hoffman, J. S., and Dendy, S.: Oceanic forcing of penultimate deglacial and last interglacial sea-level rise. *Nature*, 577(7792), 660–664. <https://doi.org/10.1038/s41586-020-1931-7>, 2020

~~18~~20. Condron, A., & Winsor, P.: Meltwater routing and the Younger Dryas. *Proceedings of the National Academy of Sciences*, 109(49), 19928–19933, <https://doi.org/10.1073/pnas.1207381109>, 2012

~~19~~21. Crosta, X., Kohfeld, K. E., Bostock, H. C., Chadwick, M., Du Vivier, A., Esper, O., Etourneau, J., Jones, J., Leventer, A., Müller, J., Rhodes, R. H., Allen, C. S., Ghadi, P., Lamping, N., Lange, C. B., Lawler, K.-A., Lund, D., Marzocchi, A., Meissner, K. J., Menviel, L., Nair, A., Patterson, M., Pike, J., Prebble, J. G., Riesselman, C., Sadatzki, H., Sime, L. C., Shukla, S. K., Thöle, L., Vorrath, M.-E., Xiao, W., and Yang, J.: Antarctic sea ice over the past 130 000 years – Part 1: a review of what proxy records tell us, *Clim. Past*, 18, 1729–1756, <https://doi.org/10.5194/cp-18-1729-2022>, 2022.

~~20~~22. Dansgaard, W., Johnsen, S. J., Clausen, H. B., Dahl-Jensen, D., Gundestrup, N. S., Hammer, C. U., Hvidberg, C. S., Steffensen, J. P., Sveinbjörnsdottir, A. E., Jouzel, J., and Bond, G.: Evidence for general instability of past climate from a 250-kyr ice-core record, *Nature*, 364, 218–220, <https://doi.org/10.1038/364218a0>, 1993

~~21~~23. Deschamps, P., Durand, N., Bard, E., Hamelin, B., Camoin, G., Thomas, A. L., Henderson, G. M., Okuno, J., and Yokoyama, Y.: Ice-sheet collapse and sea-level rise at the Bølling warming 14,600 years ago, *Nature*, 28, 559–564, <https://doi.org/10.1038/nature10902>, 2012.

~~22~~24. Golledge, N., Menviel, L., Carter, L., Fogwill, C. J., England, M. H., Cortese, G., and Levy, R. H.: Antarctic contribution to meltwater pulse 1A from reduced Southern Ocean overturning. *Nat Commun* 5, 5107, <https://doi.org/10.1038/ncomms6107>, 2014.

- [25.](#) Gomez, N., Weber, M. E., Clark, P. U., Mitrovica, J. X. and Han, H. K.: Antarctic ice dynamics amplified by Northern Hemisphere sea-level forcing, *Nature*, 587(7835), 600–604, doi:10.1038/s41586-020-2916-2, 2020
- ~~23.~~[26.](#) Goosse, H., Brovkin, V., Fichefet, T., Haarsma, R., Huybrechts, P., Jongma, J., Mouchet, A., Selten, F., Barriat, P.-Y., Campin, J.-M., Deleersnijder, E., Driesschaert, E., Goelzer, H., Janssens, I., Loutre, M.-F., Morales Maqueda, M. A., Opsteegh, T., Mathieu, P.-P., Munhoven, G., Pettersson, E. J., Renssen, H., Roche, D. M., Schaeffer, M., Tartinville, B., Timmermann, A., and Weber, S. L.: Description of the Earth system model of intermediate complexity LOVECLIM version 1.2, *Geosci. Model Dev.*, 3, 603–633, <https://doi.org/10.5194/gmd-3-603-2010>, 2010.
- ~~24.~~[27.](#) Gottschalk, J., Battaglia, G., Fischer, H., Frölicher, T. L., Jaccard, S. L., Jeltsch-Thömmes, A., Joos, F., Köhler, P., Meissner, K. J., Menviel, L., Nehrbass-Ahles, C., Schmitt, J., Schmittner, A., Skinner, L. C., and Stocker, T. F.: Mechanisms of millennial-scale atmospheric CO<sub>2</sub> change in numerical model simulations, *Quaternary Sci. Rev.*, 220, 30–74, <https://doi.org/10.1016/j.quascirev.2019.05.013>, 2019.
- ~~25.~~[28.](#) Gray, W. R., de Lavergne, C., Willis, R. C. J., Menviel, L., Spence, P., Holzer, M., Kageyama, M. and Michel, E.: Poleward Shift in the Southern Hemisphere Westerly Winds Synchronous With the Deglacial Rise in CO<sub>2</sub>, *Paleoceanography and Paleoclimatology*, 38, 7, <https://doi.org/10.1029/2023PA004666>, 2023
- ~~26.~~[29.](#) Green, R. A., Menviel, L., Meissner, K. J., Crosta, X., Chandan, D., Lohmann, G., Peltier, W. R., Shi, X., and Zhu, J.: Evaluating seasonal sea-ice cover over the Southern Ocean at the Last Glacial Maximum, *Clim. Past*, 18, 845–862, <https://doi.org/10.5194/cp-18-845-2022>, 2022.
- [30.](#) Gregoire, L. J., Payne, A. J., and Valdes, P. J.: Deglacial rapid sea level rises caused by ice-sheet saddle collapses, *Nature*, 487, 219–222, 10.1038/nature11257, 2012.
- ~~27.~~[31.](#) He, F., Shakun, J. D., Clark, P. U., Carlson, A. E., Liu, Z., Otto-Bliesner, B. L., and Kutzbach, J. E.: Northern Hemisphere forcing of Southern Hemisphere climate during the last deglaciation, *Nature*, 494, 81–85, <https://doi.org/10.1038/nature11822>, 2013.



32. He, C., Zhengyu Liu, and Aixue Hu.: The transient response of atmospheric and oceanic heat transports to anthropogenic warming. *Nature Climate Change*, 1, doi:10.1038/s41558-018-0387-3, 2019.
- 28.33. He, C., Liu, Z., Zhu, J., Zhang, J., Gu, S., Otto-Bliesner, B. L., Brady, E., Zhu, C., Jin, Y. and Sun, J.: North Atlantic subsurface temperature response controlled by effective freshwater input in “Heinrich” events, *Earth and Planetary Science Letters*, 539, 116247, <https://doi.org/10.1016/j.epsl.2020.116247>, 2020.
- 29.34. He, C., Liu, Z., Otto-Bliesner, B. L., Brady, E. C., Zhu, C., Tomas, R., Bao, Y.: Hydroclimate footprint of pan-Asian monsoon water isotope during the last deglaciation. *Science Advances*, 7(4), 1–12. <https://doi.org/10.1126/sciadv.abe2611>, 2021.
- 30.35. Hunter, S. J., Haywood, A. M., Dolan, A. M., and Tindall, J. C.: The HadCM3 contribution to PlioMIP phase 2, *Clim. Past*, 15, 1691–1713, <https://doi.org/10.5194/cp-15-1691-2019>, 2019.
- 31.36. Ivanovic, R. F., Gregoire, L. J., Kageyama, M., Roche, D. M., Valdes, P. J., Burke, A., Drummond, R., Peltier, W. R., and Tarasov, L.: Transient climate simulations of the deglaciation 21–9 thousand years before present (version 1) – PMIP4 Core experiment design and boundary conditions, *Geosci. Model Dev.*, 9, 2563–2587, <https://doi.org/10.5194/gmd-9-2563-2016>, 2016.
- 32.37. Ivanovic, R. F., Gregoire, L. J., Burke, A., Wickert, A. D., and Valdes, P. J.: Acceleration of Northern Ice Sheet Melt Induces AMOC Slowdown and Northern Cooling in Simulations of the Early Last Deglaciation, *Paleoceanography and Paleoclimatology*. 807–824. doi:10.1029/2017PA003308, 2018
- 33.38. Jouzel, J., Masson-Delmotte, V., Cattani, O., Dreyfus, G., Falourd, S., Hoffmann, G., Minster, B., Nouet, J., Barnola, J. M., Chappellaz, J., Fischer, H., Gallet, J. C., Johnsen, S., Leuenberger, M., Loulergue, L., Luethi, D., Oerter, H., Parrenin, F., Raisbeck, G., Raynaud, D., Schilt, A., Schwander, J., Selmo, E., Souchez, R., Spahni, R., Stauffer, B., Steffensen, J. P., Stenni, B., Stocker, T. F., Tison, J. L., Werner, M., and Wolff, E. W.: Orbital and Millennial Antarctic Climate Variability over the Past 800,000 Years, *Science*, 317, 793-796, <https://doi.org/10.1126/science.1141038>, 2007.
- 34.39. Kageyama, M., Merkel, U., Otto-Bliesner, B., Prange, M., Abe-Ouchi, A., Lohmann, G., Ohgaito, R., Roche, D. M., Singarayer, J., Swingedouw, D., and X Zhang: Climatic impacts of fresh water

hosing under Last Glacial Maximum conditions: a multi-model study, *Clim. Past*, 9, 935–953, <https://doi.org/10.5194/cp-9-935-2013>, 2013.

~~35-40.~~ Kageyama, M., Braconnot, P., Harrison, S. P., Haywood, A. M., Jungclaus, J. H., Otto-Bliesner, B. L., Peterschmitt, J.-Y., Abe-Ouchi, A., Albani, S., Bartlein, P. J., Brierley, C., Crucifix, M., Dolan, A., Fernandez-Donado, L., Fischer, H., Hopcroft, P. O., Ivanovic, R. F., Lambert, F., Lunt, D. J., Mahowald, N. M., Peltier, W. R., Phipps, S. J., Roche, D. M., Schmidt, G. A., Tarasov, L., Valdes, P. J., Zhang, Q., and Zhou, T.: The PMIP4 contribution to CMIP6 – Part 1: Overview and overarching analysis plan, *Geosci. Model Dev.*, 11, 1033–1057, <https://doi.org/10.5194/gmd-11-1033-2018>, 2018.

~~36-41.~~ Kageyama, M., Harrison, S. P., Kapsch, M.-L., Lofverstrom, M., Lora, J. M., Mikolajewicz, U., Sherriff-Tadano, S., Vadsaria, T., Abe-Ouchi, A., Bouttes, N., Chandan, D., Gregoire, L. J., Ivanovic, R. F., Izumi, K., LeGrande, A. N., Lhardy, F., Lohmann, G., Morozova, P. A., Ohgaito, R., Paul, A., Peltier, W. R., Poulsen, C. J., Quiquet, A., Roche, D. M., Shi, X., Tierney, J. E., Valdes, P. J., Volodin, E., and Zhu, J.: The PMIP4 Last Glacial Maximum experiments: preliminary results and comparison with the PMIP3 simulations, *Clim. Past*, 17, 1065–1089, <https://doi.org/10.5194/cp-17-1065-2021>, 2021.

~~37-42.~~ Kapsch, M.-L., Mikolajewicz, U., Ziemann, F. and Schannwell, C.: Ocean response in transient simulations of the last deglaciation dominated by underlying ice-sheet reconstruction and method of meltwater distribution, *Geophysical Research Letters*, 49, e2021GL096767, <https://doi.org/10.1029/2021GL096767>, 2022.

~~43.~~ Kobayashi, H., Oka, A., Yamamoto, A., and Abe-Ouchi, A.: Glacial carbon cycle changes by Southern Ocean processes with sedimentary amplification. *Science Advances*, 7(35), doi: [10.1126/sciadv.abg7723](https://doi.org/10.1126/sciadv.abg7723), 2021.

~~44.~~ Kobayashi, H., Oka, A., Obase, T., and Abe-Ouchi, A.: Assessing transient changes in the ocean carbon cycle during the last deglaciation through carbon isotope modeling, *Clim. Past*, 20, 769–787, <https://doi.org/10.5194/cp-20-769-2024>, 2024.

- 38.45. Kuniyoshi, Y., Abe-Ouchi, A., Sherriff-Tadano, S., Chan, W.-L., and Saito, F.: Effect of Climatic Precession on Dansgaard-Oeschger-Like Oscillations. *Geophysical Research Letters*, 49(6), e2021GL095695. <https://doi.org/10.1029/2021GL095695>, 2022.
- ~~39.1. Kobayashi, H., Oka, A., Yamamoto, A., and Abe-Ouchi, A.: Glacial carbon cycle changes by Southern Ocean processes with sedimentary amplification. *Science Advances*, 7(35), doi: 10.1126/sciadv.abg7723, 2021.~~
- 40.46. Lambeck, K., Rouby, H., Purcell, A., Sun, Y., and Sambridge, M.: Sea level and global ice volumes from the Last Glacial Maximum to the Holocene, *P. Natl. Acad. Sci.*, 111, 15296–15303, 10.1073/pnas.1411762111, 2014.
- 41.47. Lhardy, F., Bouttes, N., Roche, D. M., Crosta, X., Waelbroeck, C., and Paillard, D.: Impact of Southern Ocean surface conditions on deep ocean circulation during the LGM: a model analysis, *Clim. Past*, 17, 1139–1159, <https://doi.org/10.5194/cp-17-1139-2021>, 2021.
- 42.48. Lisiecki, L. E. and Raymo, M. E.: A Pliocene-Pleistocene stack of 57 globally distributed benthic  $\delta^{18}\text{O}$  records, *Paleoceanography*, 20, PA1003, doi:10.1029/2004PA001071, 2005
49. Liu, Z., Otto-Bliesner, B. L., He, F., Brady, E. C., Tomas, R., Clark, P. U., Carlson, A. E., Lynch-Stieglitz, J., Curry, W., Brook, E., Erickson, D., Jacob, R., Kutzbach, J., and Cheng, J.: Transient Simulation of Last Deglaciation with a New Mechanism for Bølling-Allerød Warming, *Science*, 325, 310–314, doi:10.1126/science.1171041, 2009
50. Liu, Z., Bao, Y., Thompson, L. G., Mosley-Thompson, E., Tabor, C., Zhang, G. J., Yan, M., Lofverstrom, M., Montanez, I., and Oster, J.: Tropical mountain ice core  $\delta^{18}\text{O}$ : A Goldilocks indicator for global temperature change, *Science Advances*, 9, 45, <https://doi.org/10.1126/sciadv.adi6725>, 2023
- 43.51. Love, R., Andres, H. J., Condon, A., and Tarasov, L.: Freshwater routing in eddy-permitting simulations of the last deglacial: the impact of realistic freshwater discharge, *Clim. Past*, 17, 2327–2341, <https://doi.org/10.5194/cp-17-2327-2021>, 2021.
- 44.52. Lowry, D. P., Golledge, N. R., Menviel, L., and Bertler, N. A. N.: Deglacial evolution of regional Antarctic climate and Southern Ocean conditions in transient climate simulations. 189–215, 2018.

962 ~~45.53.~~ Lynch-Stieglitz, J., Adkins, J. F., Curry, W. B., Dokken, T., Hall, I. R., Herguera, J. C. and Zahn,  
963 R.: Atlantic meridional overturning circulation during the Last Glacial Maximum. *Science*,  
964 316(5821), 66–69. <https://doi.org/10.1126/science.1137127>, 2007

965 ~~46.54.~~ MacDougall, A. H., Frölicher, T. L., Jones, C. D., Rogelj, J., Matthews, H. D., Zickfeld, K., Arora,  
966 V. K., Barrett, N. J., Brovkin, V., Burger, F. A., Eby, M., Eliseev, A. V., Hajima, T., Holden, P. B.,  
967 Jeltsch-Thömmes, A., Koven, C., Mengis, N., Menviel, L., Michou, M., Mokhov, I. I., Oka, A.,  
968 Schwinger, J., Séférian, R., Shaffer, G., Sokolov, A., Tachiiri, K., Tjiputra, J., Wiltshire, A., and  
969 Ziehn, T.: Is there warming in the pipeline? A multi-model analysis of the Zero Emissions  
970 Commitment from CO<sub>2</sub>, *Biogeosciences*, 17, 2987–3016, <https://doi.org/10.5194/bg-17-2987-2020>,  
971 2020.

972 ~~47.55.~~ Marcott, S. A., Bauska, T. K., Buizert, C., Steig, E. J., Rosen, J. L., Cuffey, K. M., Fudge, T. J.,  
973 Severinghaus, J. P., Kalk, M. L., McConnell, J. R., Sowers, T., Taylor, K. C. White, J. W. C. and  
974 Brook, E. J.: Centennial-scale changes in the global carbon cycle during the last deglaciation. *Nature*,  
975 514(7524), 616–619. <https://doi.org/10.1038/nature13799>, 2014

976 ~~48.56.~~ Margari, V., Skinner, L. C., Menviel, L., Capron, E., Rhodes, R. H., Martrat, B., and Grimalt, J.  
977 O.: Fast and slow components of interstadial warming in the North Atlantic during the last glacial.  
978 *Communications Earth & Environment*, 1–9. <https://doi.org/10.1038/s43247-020-0006-x>, 2020

979 ~~49.57.~~ Mariotti, V., Paillard, D., Bopp, L., Roche, D. M., and Bouttes, N.: A coupled model for carbon  
980 and radiocarbon evolution during the last deglaciation. *Geophysical Research Letters*, 43(3), 1306–  
981 1313. <https://doi.org/10.1002/2015GL067489>, 2016.

982 ~~50.58.~~ Marson, J. M., Mysak, L. A., Mata, M. M., and Wainer, I.: Evolution of the deep Atlantic water  
983 masses since the last glacial maximum based on a transient run of NCAR-CCSM3. *Climate Dynamics*,  
984 47(3–4), 865–877. <https://doi.org/10.1007/s00382-015-2876-7>, 2016

985 ~~51.59.~~ Martínez-García, A., Rosell-Melé, A., Jaccard, S.: Southern Ocean dust–climate coupling over  
986 the past four million years. *Nature* 476, 312–315. <https://doi.org/10.1038/nature10310>, 2011.

987 ~~52.60.~~ Martrat, B., Grimalt, J. O., Shackleton, N. J., de Abreu, L., Hutterli, M.A., and Stocker, T. F.: Four  
988 climate cycles of recurring deep and surface water destabilizations on the Iberian Margin, *Science*,  
989 317, 502–507, doi:10.1126/science.1139994, 2007.

990 [61.](#) Marzocchi, A. and Jansen, M. F. Global cooling linked to increased glacial carbon storage via  
 991 changes in Antarctic sea ice. *Nature Geoscience*, 12, 1001–1005, [https://doi.org/10.1038/s41561-](https://doi.org/10.1038/s41561-019-0466-8)  
 992 019-0466-8, 2019

993 ~~53.~~[62.](#) Masoum, A., Nerger, L., Willeit, M., Ganopolski, A., and Lohmann, G.: *Lessons From Transient*  
 994 *Simulations of the Last Deglaciation With CLIMBER-X: GLAC1D Versus PaleoMist*, *Geophysical*  
 995 *Research Letters*, 51(16), e2023GL107310. <https://doi.org/10.1029/2023GL107310>, 2024.

996 ~~54.~~[63.](#) McManus, J. F., Francois, R., Gherardi, J.-M., Keigwin, L. D., and Brown-Leger, S.: Collapse  
 997 and rapid resumption of Atlantic meridional circulation linked to deglacial climate changes, *Nature*,  
 998 428, 834–837, 10.1038/nature02494, 2004.

999 ~~55.~~[64.](#) Menviel, L., Yu, J., Joos, F., Mouchet, A., Meissner, K. J., and England, M. H.: Poorly ventilated  
 1000 deep ocean at the Last Glacial Maximum inferred from carbon isotopes: A data-model comparison  
 1001 study. *Paleoceanography*, 32(1), 2–17. <https://doi.org/10.1002/2016PA003024>, 2017.

1002 ~~56.~~[65.](#) Menviel, L., Timmermann, a., Timm, O. E., and Mouchet, A.: Climate and biogeochemical  
 1003 response to a rapid melting of the West Antarctic Ice sheet during interglacials and implications for  
 1004 future climate. *Paleoceanography*, 25, 1–12. <https://doi.org/10.1029/2009PA001892>, 2010.

1005 ~~57.~~[66.](#) Menviel, L., Timmermann, A., Timm, O. E., and Mouchet, A.: Deconstructing the Last Glacial  
 1006 termination: the role of millennial and orbital-scale forcings, *Quaternary Sci. Rev.*, 30, 1155–1172,  
 1007 10.1016/j.quascirev.2011.02.005, 2011.

1008 ~~58.~~[67.](#) Menviel, L., England, M. H., Meissner, K. J., Mouchet, A., and Yu, J.: Atlantic-Pacific seesaw  
 1009 and its role in outgassing CO<sub>2</sub> during Heinrich events. *Paleoceanography*, 29(January), 58–70.  
 1010 <https://doi.org/10.1002/2013PA002542>, 2014.

1011 ~~59.~~[68.](#) Menviel, L., Spence, P., Yu, J., Chamberlain, M. A., Matear, R. J., Meissner, K. J., and England,  
 1012 M. H.: Southern Hemisphere westerlies as a driver of the early deglacial atmospheric CO<sub>2</sub> rise.  
 1013 *Nature Communications*, 9(1), 1–12. <https://doi.org/10.1038/s41467-018-04876-4>, 2018

1014 ~~60.~~[69.](#) Moros, M., De Deckker, P., Perner, K., Ninnemann, U. S., Wacker, L., Telford, R., Jansen, E.,  
 1015 Blanz, T. and Schneider, R.: Hydrographic shifts south of Australia over the last deglaciation and  
 1016 possible interhemispheric linkages. *Quaternary Research (United States)*, 102, 130–141.  
 1017 <https://doi.org/10.1017/qua.2021.12>, 2021

1018 ~~61~~70. Moy, A. D., Palmer, M. R., Howard, W. R., Bijma, J., Cooper, M. J., Calvo, E., Pelejero, C.,  
1019 Gagan, M. K. and Chalk, T. B.: Varied contribution of the Southern Ocean to deglacial atmospheric  
1020 CO<sub>2</sub> rise. *Nature Geoscience*, 12(12), 1006–1011. <https://doi.org/10.1038/s41561-019-0473-9>, 2019

1021 ~~62~~71. Ng, H. C., Robinson, L. F., McManus, J. F., Mohamed, K. J., Jacobel, A. W., Ivanovic, R. F.,  
1022 Gregoire, L. J. and Chen, T.: Coherent deglacial changes in western Atlantic Ocean circulation.  
1023 *Nature Communications*, 9(1), 1–10. <https://doi.org/10.1038/s41467-018-05312-3>, 2018

1024 ~~63~~72. Obase, T., and Abe- Ouchi, A.: Abrupt Bølling-Allerød warming simulated under gradual forcing  
1025 of the last deglaciation, *Geophysical Research Letters*, 46, <https://doi.org/10.1029/2019GL084675>,  
1026 2019.

1027 ~~64~~73. Obase, T., A. Abe-Ouchi, F. Saito: Abrupt climate changes in the last two deglaciations simulated  
1028 with different Northern ice sheet discharge and insolation, *Scientific Reports*, 11, doi:  
1029 10.1038/s41598-021-01651-2, 2021

1030 ~~65~~74. Parrenin, F., Masson-Delmotte, V., Köhler, P., Raynaud, D., Paillard, D., Schwander, J., Barbante,  
1031 C., Landais, A., Wegner, A., Jouzel, J.: Atmospheric carbon dioxide, methane, deuterium, and  
1032 calculated Antarctic temperature of EPICA Dome C ice core. *PANGAEA*,  
1033 doi:10.1594/PANGAEA.810199, 2013

1034 ~~66~~75. Pedro, J. B., Martin, T., Steig, E. J., Jochum, M., Park, W., & Rasmussen, S. O.: Southern Ocean  
1035 deep convection as a driver of Antarctic warming events. *Geophysical Research Letters*, 43(5), 2192–  
1036 2199. <https://doi.org/10.1002/2016GL067861>, 2016

1037 ~~67~~76. Pedro, J. B., Jochum, M., Buizert, C., He, F., Barker, S., & Rasmussen, S. O.: Beyond the bipolar  
1038 seesaw: Toward a process understanding of interhemispheric coupling. *Quaternary Science Reviews*,  
1039 192, 27–46. <https://doi.org/10.1016/j.quascirev.2018.05.005>, 2018

1040 ~~68~~77. Peltier, W. R., Argus, D. F., and Drummond, R.: Space geodesy constrains ice age terminal  
1041 deglaciation: The global ICE-6G\_C (VM5a) model, *J. Geophys. Res.-Sol. Ea.*, 120, 450–487,  
1042 10.1002/2014JB011176, 2015.

1043 ~~69~~78. Petit, J. R., Jouzel, J., Raynaud, D., Barkov, N. I., Barnola, J.-M., Basile, I., Bender, M.,  
1044 Chappellaz, J., Davis, M., Delaygue, G., Delmotte, M., Kotlyakov, V. M., Legrand, M., Lipenkov,  
1045 V. Y., Lorius, C., PÉpin, L., Ritz, C., Saltzman, E., and Stievenard, M.: Climate and atmospheric

history of the past 420 000 years from the Vostok ice core, Antarctica, *Nature*, 399, 429–436, 10.1038/20859, 1999.

[79.](#) Pöppelmeier, F., Jeltsch-Thömmes, A., Lippold, J. et al. Multi-proxy constraints on Atlantic circulation dynamics since the last ice age. *Nat. Geosci.* 16, 349–356 (2023). <https://doi.org/10.1038/s41561-023-01140-3>

~~70.~~[80.](#) Prange, M., Jonkers, L., Merkel, U., Schulz, M. and Bakker, P: A multicentennial mode of North Atlantic climate variability throughout the Last Glacial Maximum, *Science*, 9, 44, <https://www.science.org/doi/10.1126/sciadv.adh1106>, 2023.

~~71.~~[81.](#) Rae, J. W. B., Burke, A., Robinson, L. F., Adkins, J. F., Chen, T., Cole, C., Greenop, R., Li, T., Littley, E. F. M., Nita, D. C., Stewart, J. A. and Taylor, B. J.: CO<sub>2</sub> storage and release in the deep Southern Ocean on millennial to centennial timescales, *Nature*, 562, 569–573, <https://doi.org/10.1038/s41586-018-0614-0>, 2018

~~72.~~[82.](#) Renssen, H., Mairesse, A., Goosse, H., Mathiot, P., Heiri, O., Roche, D. M., Nisancioglu, K. H. and Valdes, P. J.: Multiple causes of the Younger Dryas cold period. *Nature Geoscience*, 8(12), 946–949. <https://doi.org/10.1038/ngeo2557>, 2015

~~73.~~[83.](#) Roberts, N. L., Piotrowski, A. M., McManus, J. F., and Keigwin, L. D.: Synchronous Deglacial Overturning and Water Mass Source Changes, *Science*, 327, 75–78, 10.1126/science.1178068, 2010.

[84.](#) Roche, D. M., Renssen, H., Paillard, D., & Levavasseur, G.: Deciphering the spatio-temporal complexity of climate change of the last deglaciation: A model analysis. *Climate of the Past*, 7(2), 591–602. <https://doi.org/10.5194/cp-7-591-2011>, 2011

~~74.~~[85.](#) Roche, D.M., Wiersma, A.P. & Renssen, H. A systematic study of the impact of freshwater pulses with respect to different geographical locations. *Clim Dyn* 34, 997–1013. <https://doi.org/10.1007/s00382-009-0578-8>, 2010.

[86.](#) Rojas, M., Moreno, P., Kageyama, M., Crucifix, M., Hewitt, C., Abe-Ouchi, A., Ohgaito, R., Brady E. C. and Hope, P.: The Southern Westerlies during the last glacial maximum in PMIP2 simulations. *Climate Dynamics*, 32(4), 525–548. <https://doi.org/10.1007/s00382-008-0421-7>, 2009



87. [Sadatzki, H., Opdyke, B., Menviel, L., Leventer, A., Hope, J. M., Brocks, J. J., Fallon, S., Post, A. L., O'Brien, P. E., Grant, K., & Armand, L.: Early sea ice decline off East Antarctica at the last glacial-interglacial climate transition, \*Science Advances\*, 9, 41, doi: 10.1126/sciadv.adh9513, 2023.](#)
- ~~75~~88. [Schloesser, F., Friedrich, T., Timmermann, A., DeConto, R. M., and Pollard, D.: Antarctic iceberg impacts on future Southern Hemisphere climate, \*Nat. Clim. Change\*, 9, 672–677, <https://doi.org/10.1038/s41558-019-0546-1>, 2019.](#)
- ~~76~~89. [Seroussi, H., Nowicki, S., Payne, A. J., Goelzer, H., Lipscomb, W. H., Abe-Ouchi, A., Agosta, C., Albrecht, T., Asay-Davis, X., Barthel, A., Calov, R., Cullather, R., Dumas, C., Galton-Fenzi, B. K., Gladstone, R., Golledge, N. R., Gregory, J. M., Greve, R., Hattermann, T., Hoffman, M. J., Humbert, A., Huybrechts, P., Jourdain, N. C., Kleiner, T., Larour, E., Leguy, G. R., Lowry, D. P., Little, C. M., Morlighem, M., Pattyn, F., Pelle, T., Price, S. F., Quiquet, A., Reese, R., Schlegel, N.-J., Shepherd, A., Simon, E., Smith, R. S., Straneo, F., Sun, S., Trusel, L. D., Van Breedam, J., van de Wal, R. S. W., Winkelmann, R., Zhao, C., Zhang, T., and Zwinger, T.: ISMIP6 Antarctica: a multi-model ensemble of the Antarctic ice sheet evolution over the 21st century, \*The Cryosphere\*, 14, 3033–3070, <https://doi.org/10.5194/tc-14-3033-2020>, 2020.](#)
- ~~77~~90. [Severinghaus, J. P. and Brook, E. J.: Abrupt Climate Change at the End of the Last Glacial Period Inferred from Trapped Air in Polar Ice, \*Science\*, 286, 930–934, 10.1126/science.286.5441.930, 1999.](#)
- ~~78~~91. [Shakun, J. D., Clark, P. U., He, F., Marcott, S. A., Mix, A. C., Liu, Z., Otto-Bliesner, B., Schmittner, A., and Bard, E.: Global warming preceded by increasing carbon dioxide concentrations during the last deglaciation, \*Nature\*, 484, 49–54, 10.1038/nature10915, 2012.](#)
- ~~79~~92. [Sherriff-Tadano, S., Abe-Ouchi, A., Yoshimori, M., Ohgaito, R., Vadsaria, T., Chan, W-L., Hotta, H., Kikuchi, M., Kodama, T., Oka, A., Southern Ocean surface temperatures and cloud biases in climate models connected to the representation of glacial deep ocean circulation, \*Journal of Climate\*. 3849–3866, <https://doi.org/10.1175/JCLI-D-22-0221.1>, 2023](#)
- ~~80~~93. [Sigman, D. M., Hain, M. P., & Haug, G. H.: The polar ocean and glacial cycles in atmospheric CO2 concentration. \*Nature\*, 466\(7302\), 47–55. <https://doi.org/10.1038/nature09149>, 2010](#)
- ~~81~~94. [Sikes, E. L., Schiraldi, B., & Williams, A.: Seasonal and Latitudinal Response of New Zealand Sea Surface Temperature to Warming Climate Since the Last Glaciation: Comparing Alkenones to](#)

Mg/Ca Foraminiferal Reconstructions. *Paleoceanography and Paleoclimatology*, 34(11), 1816–1832.  
<https://doi.org/10.1029/2019PA003649>, 2019.

~~82-95.~~ Sime, L. C., Kohfeld, K. E., Le, C., Wolff, E. W., Boer, A. M. De, Graham, R. M., & Bopp, L.: Southern Hemisphere westerly wind changes during the Last Glacial Maximum: model-data comparison. *Quaternary Science Reviews*, 64, 104–120.  
<https://doi.org/10.1016/j.quascirev.2012.12.008>, 2013.

~~83-96.~~ Skinner, L. C., Fallon, S., Waelbroeck, C., Michel, E., & Barker, S.: Ventilation of the deep Southern Ocean and deglacial CO<sub>2</sub> rise. *Science*, 328(5982), 1147–1151.  
<https://doi.org/10.1126/science.1183627>, 2010

~~97.~~ Snoll, B., Ivanovic, R.F., Valdes, P.J., Maycock, A. C. and Gregoire, L. J.: Effect of orographic gravity wave drag on Northern Hemisphere climate in transient simulations of the last deglaciation. *Clim Dyn* 59, 2067–2079. <https://doi.org/10.1007/s00382-022-06196-2>, 2022.

~~84-98.~~ [Snoll, B., Ivanovic, R., Gregoire, L., Sherriff-Tadano, S., Menviel, L., Obase, T., Abe-Ouchi, A., Bouttes, N., He, C., He, F., Kapsch, M., Mikolajewicz, U., Muglia, J., and Valdes, P.: A multi-model assessment of the early last deglaciation \(PMIP4 LDv1\): a meltwater perspective, \*Clim. Past\*, 20, 789–815, <https://doi.org/10.5194/cp-20-789-2024>, 2024.](#)

~~85-99.~~ Steffensen, J. P., Andersen, K. K., Bigler, M., Clausen, H. B., Dahl-Jensen, D., Fischer, H., Goto-Azuma, K., Hansson, M., Johnsen, S. J., Jouzel, J., Masson-Delmotte, V., Popp, T., Rasmussen, S. O., Röthlisberger, R., Ruth, U., Stauffer, B., Siggaard-Andersen, M.-L., Sveinbjörnsdóttir, Á. E., Svensson, A., and White, J. W. C.: High-Resolution Greenland Ice Core Data Show Abrupt Climate Change Happens in Few Years, *Science*, 321, 680–684, [10.1126/science.1157707](https://doi.org/10.1126/science.1157707), 2008.

~~86-100.~~ Stein, K., Timmermann, A., Young Kwon, E., and Friedrich, T.: Timing and magnitude of Southern Ocean sea ice/carbon cycle feedbacks, *P. Natl. Acad. Sci. USA*, 117, 9, <https://doi.org/10.1073/pnas.1908670117>, 2020.

~~87-101.~~ Stocker, T. F., & Johnsen, S. J.: A minimum thermodynamic model for the bipolar seesaw. *Paleoceanography*, 18(4), 1–9. <https://doi.org/10.1029/2003PA000920>, 2003

1126 ~~88~~102. Stouffer, R. J., Yin, J., Gregory, J. M., Dixon, K. W., & Spelman, M. J.: Investigating the  
 1127 Causes of the Response of the Thermohaline Circulation to Past and. *Journal of Climate*, 19, 1365–  
 1128 1387. <https://doi.org/10.1002/9781119115397.ch25>, 2006

1129 ~~89~~103. Tarasov, L., Dyke, A. S., Neal, R. M., and Peltier, W. R.: A data-calibrated distribution of  
 1130 deglacial chronologies for the North American ice complex from glaciological modeling, *Earth*  
 1131 *Planet. Sci. Lett.*, 315–316, 30–40, 10.1016/j.epsl.2011.09.010, 2012

1132 ~~90~~104. Tierney, J. E., Zhu, J., King, J., Malevich, S. B., Hakim, G. J., & Poulsen, C. J.: Glacial  
 1133 cooling and climate sensitivity revisited. *Nature*, 584(7822), 569–573.  
 1134 <https://doi.org/10.1038/s41586-020-2617-x>, 2020

1135 ~~94~~105. Timmermann, A., Timm, O., Stott, L., and Menviel, L.: The roles of CO<sub>2</sub> and orbital  
 1136 forcing in driving Southern Hemispheric temperature variations during the last 21 000 Yr. *Journal of*  
 1137 *Climate*, 22(7), 1626–1640. <https://doi.org/10.1175/2008JCLI2161.1>, 2009

1138 ~~92~~106. Toucanne, S., Zaragosi, S., Bourillet, J.-F., Marieu, V., Cremer, M., Kageyama, M., Van  
 1139 Vliet-Lanoë, B., Eynaud, F., Turon, J.-L., and Gibbard, P.-L.: The first estimation of Fleuve Manche  
 1140 palaeoriver discharge during the last deglaciation: Evidence for Fennoscandian ice sheet meltwater  
 1141 flow in the English Channel ca 20–18 ka ago, *Earth Planet. Sc. Lett.*, 290, 459–473, 2010.

1142 ~~93~~107. WAIS Divide Project Members: Onset of deglacial warming in West Antarctica driven by  
 1143 local orbital forcing. *Nature*, 500(7463), 440–444. <https://doi.org/10.1038/nature12376>, 2013.

1144 108. WAIS Divide project members: Precise interpolar phasing of abrupt climate change during the last  
 1145 ice age. *Nature*, 520(7549), 661–665. <https://doi.org/10.1038/nature14401>, 2015

1146 ~~94~~109. [Weitzel, N., Andres, H., Baudouin, J.-P., Kapsch, M.-L., Mikolajewicz, U., Jonkers, L.,  
 1147 Bothe, O., Ziegler, E., Kleinen, T., Paul, A., and Rehfeld, K.: Towards spatio-temporal comparison  
 1148 of simulated and reconstructed sea surface temperatures for the last deglaciation, \*Clim. Past\*, 20, 865–  
 1149 890, <https://doi.org/10.5194/cp-20-865-2024>, 2024.](#)

1150 ~~95~~110. Yoshimori, M., Yokohata, T., and Abe-Ouchi, A.: A Comparison of Climate Feedback  
 1151 Strength between CO<sub>2</sub> Doubling and LGM Experiments, *J. Climate*, 22, 3374–3395,  
 1152 <https://doi.org/10.1175/2009JCLI2801.1>, 2009.

1153 ~~96~~111. Zhu, J. and Poulsen, C. J.: Last Glacial Maximum (LGM) climate forcing and ocean  
1154 dynamical feedback and their implications for estimating climate sensitivity, *Clim. Past*, 17, 253–  
1155 267, <https://doi.org/10.5194/cp-17-253-2021>, 2021.  
1156  
1157